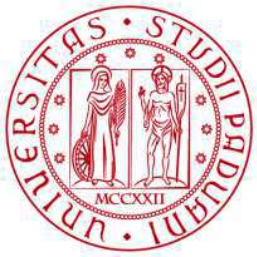

UNIVERSITÀ DEGLI STUDI DI PADOVA

UNIVERSITA' DEGLI STUDI DI PADOVA

Dipartimento di Ingegneria Industriale DII

Corso di Laurea Magistrale in Ingegneria Energetica

Design optimization and energy assessment of coaxial geothermal heat exchangers for residential applications

Relatore:

Prof. MICHELE De Carli

Correlatori:

Ing. Nicola Mutinelli

Ing. Mattia Chinello

Studente con Matricola

Behzad Ghorbani – 2070920

Anno Accademico 2024/2025

Acknowledgment

I would like to express my deepest appreciation to my academic supervisor, Professor De Carli, from the University of Padova, for his valuable guidance and continuous support throughout the development of my thesis.

I am also sincerely grateful to Eng. Nicola Mutinelli and Eng. Mattia Chinello, my supervisors at RED S.R.L., where I had the opportunity to carry out this thesis as part of an internship. Their technical insights, encouragement, and mentorship played a crucial role in shaping the outcome of this work.

I extend heartfelt thanks to my family for their unwavering love, patience, and belief in my potential. Their support has been a cornerstone throughout my academic journey.

To my friends, who provided constant motivation, empathy, and strength during challenging moments, I offer my sincere appreciation.

To everyone who contributed to this achievement in any capacity, I am truly grateful. Your presence has made this experience both meaningful and memorable.

Padova, July 2025

Behzad Ghorbani

Abstract

The Department of Industrial Engineering at the University of Padua emphasizes the importance of advancing sustainable thermal energy systems. This thesis work was carried out in collaboration with RED Srl (Renewable Energy Development), an industrial partner operating in the geothermal sector. The study investigates the thermal performance of shallow coaxial geothermal heat exchangers (CGHEs), focusing on the impact of varying inner and outer pipe diameters. The entire study is contextualized within the climatic and soil conditions of Padua, northern Italy, where the system is intended to supply thermal energy to residential buildings.

A preliminary numerical simulation study was carried out using COMSOL Multiphysics to determine how different pipe configurations affect thermal efficiency and outlet fluid temperature under steady-state winter operation. To ensure model reliability, the simulations were validated using real-world data collected from a geothermal system located in Putte, Belgium, provided by RED Srl. Validation was performed by comparing the numerical output with measured data and evaluating the tolerance range according to ASHRAE guidelines.

In this study, several coaxial configurations were tested across different diameter ratios. Once validated, the results were applied in Termus and Geotermus software environments to assess energy demands for residential building projects under the local conditions of Padua. By simulating insulation changes in building components (walls, windows, roofs), the minimum required drilling depth to meet seasonal energy demand was recalculated.

The findings of this work demonstrate that optimizing the pipe geometry can significantly enhance system performance, reduce required drilling depth, and improve seasonal efficiency. The study confirms that shallow coaxial geothermal systems are highly suitable for heating applications that require moderate temperatures, such as residential heating in Italy, and offers practical design insights to guide future system optimization.

Sommario

Il Dipartimento di Ingegneria Industriale dell'Università di Padova sottolinea l'importanza dello sviluppo di sistemi energetici termici sostenibili. Il presente lavoro di tesi è stato svolto in collaborazione con l'azienda RED Srl (Renewable Energy Development), attiva nel settore geotermico. La tesi analizza le prestazioni termiche di scambiatori di calore geotermici coassiali a bassa profondità (CGHE), con particolare attenzione all'influenza delle variazioni del diametro interno ed esterno delle tubazioni. L'intero studio è contestualizzato nelle condizioni climatiche e geologiche di Padova, nel nord Italia, dove il sistema è destinato alla climatizzazione di edifici ad uso residenziale.

Uno studio preliminare di simulazione numerica è stato condotto utilizzando COMSOL Multiphysics per valutare come diverse configurazioni geometriche influenzino l'efficienza termica e la temperatura in uscita del fluido durante l'operazione invernale in regime stazionario. Per garantire l'affidabilità del modello, i risultati delle simulazioni sono stati validati mediante dati reali forniti da RED Srl, provenienti da un impianto geotermico situato a Putte, in Belgio. La validazione è stata effettuata confrontando i risultati numerici con i dati misurati e verificando il margine di tolleranza secondo le linee guida ASHRAE.

In questo studio, sono state analizzate diverse configurazioni coassiali con differenti rapporti tra i diametri. Dopo la validazione, i risultati sono stati applicati nei software Termus Geotermus per valutare il fabbisogno energetico di edifici residenziali, tenendo conto delle condizioni locali di Padova. Simulando interventi di miglioramento dell'isolamento degli edifici (muri, infissi, coperture), è stata ricalcolata la profondità minima necessaria per soddisfare il fabbisogno energetico stagionale.

I risultati di questo lavoro dimostrano che l'ottimizzazione della geometria delle tubazioni può migliorare significativamente le prestazioni del sistema, ridurre la profondità di perforazione richiesta e aumentare l'efficienza stagionale. Lo studio conferma che i sistemi geotermici coassiali a bassa profondità sono particolarmente adatti per applicazioni a temperatura moderata in contesti residenziali, come il riscaldamento residenziale in Italia, e offre indicazioni progettuali utili per ottimizzare tali sistemi in futuro.

Nomenclature

Symbol	Description	Unit
C_w	Water specific heat capacity	$\frac{J}{kg.K}$
D_h	Hydraulic diameter	m
D_i	Inner pipe diameter	mm
D_o	Outer pipe diameter	mm
$\boldsymbol{f_D}$	Darcy friction factor	-
k	Thermal conductivity of the material	$\frac{W}{mK}$
L	Pipe length	m
L_c	Required pipe length for cooling	m
L_h	Required pipe length for heating	m
$\boldsymbol{\dot{m}}$	Mass flow rate	$\frac{kg}{s}$
Nu	Nusselt number	-
p	Pressure	Pa
P_C	Cooling power	W
P_h	Heating power	W
Q_C	Cooling energy	kWh
Q_h	Heating energy	kWh
p	Pressure	Pa
$\dot{\mathbf{Q}}$	Thermal power	W
Re	Reynolds number	-
$\boldsymbol{R_{conv}}$	Convective thermal resistance	$\frac{mK}{W}$
T	Temperature	K
t	Time	s
ρ	Density	$\frac{kg}{m^3}$

Table of Contents

List of Figures

List of Tables

1

Introduction

1.1 Thesis Overview

This thesis investigates the thermal behaviour and energy performance of shallow coaxial borehole heat exchangers (CBHEs), with a particular focus on how variations in the inner and outer pipe diameters influence overall system efficiency. The study begins with a numerical simulation model developed using COMSOL Multiphysics®, which is validated against real operational data from a geothermal installation in Putte, Belgium.

Once validated, the model is adapted to reflect the climatic and geological conditions of Padua, Italy, to analyse the impact of geometric parameters under local scenarios. The simulation results are then integrated into Termus and Geotermus software to evaluate real-world energy demands for residential buildings. This enables the determination of optimal borehole depths required to meet both heating and cooling needs.

Additionally, the thesis conducts parametric analyses to assess the influence of fluid temperature, flow rate, pipe material, and thermal short-circuiting along the borehole length.

1.2 Background and Rationale

Space heating and cooling account for nearly half of the total final energy consumption within the European Union (EU), making it the most energy-intensive sector surpassing even transport. A large share of this demand is still satisfied using fossil fuels, significantly contributing to greenhouse gas emissions.

However, in recent years, the use of renewable energy in the EU's heating and cooling sector has steadily increased, reaching 26.2% in 2023 [1]. This aligns with the EU's climate goals to cut greenhouse gas emissions by 55% by 2030 and reach net-zero by 2050 [2].

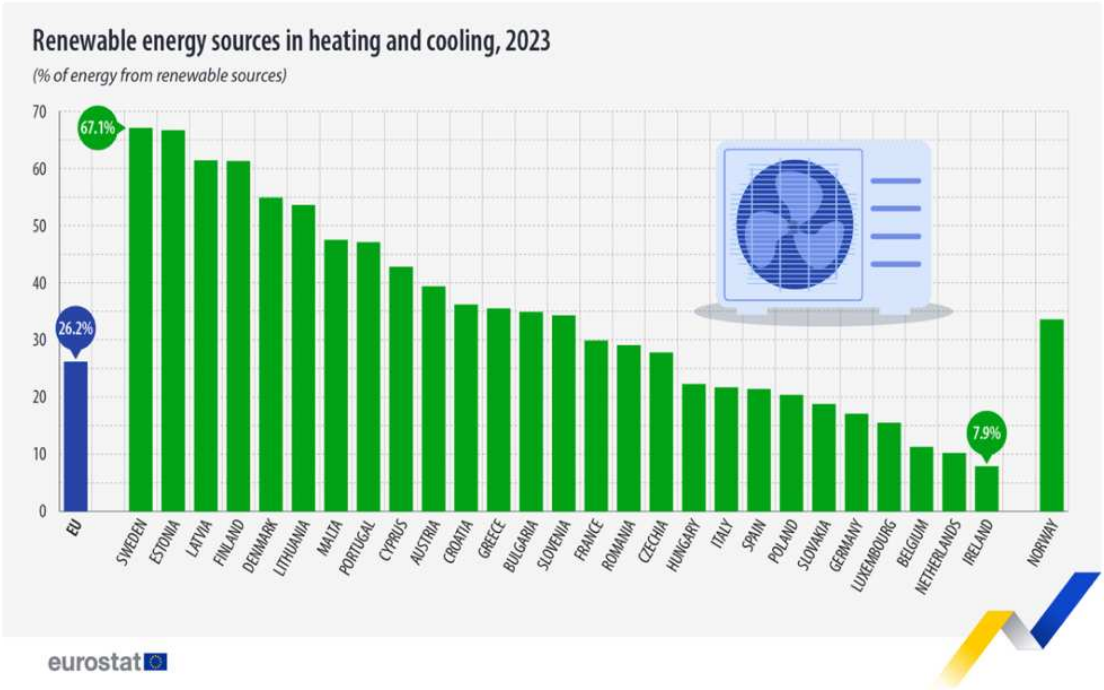

Figure 1. 1 ***Renewable energy share in heating and cooling across EU countries in 2023[1]***

Although solar and wind energy have become more widespread, they still present a key limitation: they do not provide energy continuously. Solar power functions only when the sun is shining, and wind energy depends on when and where the wind blows. As a result, these sources cannot always supply energy when it is most needed, such as during night time or calm days. While energy storage systems like batteries can offer support, current technologies are not yet capable of storing large amounts of energy over extended periods.

Therefore, it is essential to invest in renewable sources that can provide a stable and continuous energy supply, independent of weather conditions or storage requirements. Among such options, geothermal energy stands out as a highly reliable solution.

1.2.1 Importance of Geothermal Energy

Geothermal energy is one of the few renewable energy sources capable of delivering a constant and uninterrupted supply of thermal energy. Unlike solar or wind energy, which depend on weather and time of day, geothermal systems extract heat from deep within the Earth, where conditions remain stable year-round. This reliability makes geothermal energy especially suitable for applications that require consistent energy for heating or electricity production.

Historically, geothermal energy has been used in many countries for both electricity generation and direct heating. In recent years, improved technologies have expanded the use of geothermal systems

beyond traditional high-temperature zones, making them viable in a wider range of locations and for diverse purposes including residential heating and industrial operations.

Geothermal energy is generally categorized into high-enthalpy and low-enthalpy systems. High-enthalpy systems are typically found in volcanic or tectonically active regions and are used for electricity generation, with underground temperatures exceeding 150 °C [3]. In contrast, low-enthalpy (or shallow) geothermal systems operate at much lower temperatures, typically below 30 °C, and utilize the stable ground temperature found at depths of less than 100 m [4]. These shallow systems are widely used for heating and cooling buildings through ground heat exchangers. Because the term "geothermal" can refer to both categories, it is important to clarify that this thesis specifically focuses on low-enthalpy geothermal applications designed for residential thermal energy supply.

1.2.2 Limitations of Traditional Open-Loop Systems

Traditional geothermal systems often use open-loop configurations, particularly in deep (high-enthalpy) applications, where geothermal fluids are extracted from underground reservoirs, used for heating or power generation, and then reinjected into the Earth. These systems are effective but depend heavily on suitable geological conditions and can pose environmental risks, such as fluid corrosion and subsurface disturbances.

In shallow (low-enthalpy) systems, open-loop designs can still be applied by extracting groundwater from wells and reinjecting it after heat exchange. While they are generally safer and simpler than deep systems, challenges such as water availability, legal permits, and long-term sustainability may limit their use. These factors have led to increasing interest in closed-loop systems for low-enthalpy applications.

1.2.3 Development of Closed-Loop Systems

To address the limitations of open-loop systems, closed-loop geothermal technologies have gained increasing attention. The most commonly adopted closed-loop configurations include single U-tube and double U-tube systems, in which a heat-transfer fluid circulates through polyethylene pipes buried underground, transferring heat via conduction without direct contact with groundwater or soil.

Among these technologies, the coaxial borehole heat exchanger (CBHE) has emerged as a particularly promising design. CBHEs consist of two concentric pipes forming a sealed circuit where the fluid flows downward in the outer annulus and returns upward through the inner pipe. This configuration allows efficient heat exchange while simplifying installation and reducing borehole diameter compared to U-tube systems.

CBHE systems are especially suited for shallow-depth applications (typically less than 100 meters), making them ideal for urban environments or areas with limited drilling space. They offer reduced environmental impact, simpler maintenance, and reliable year-round thermal performance.

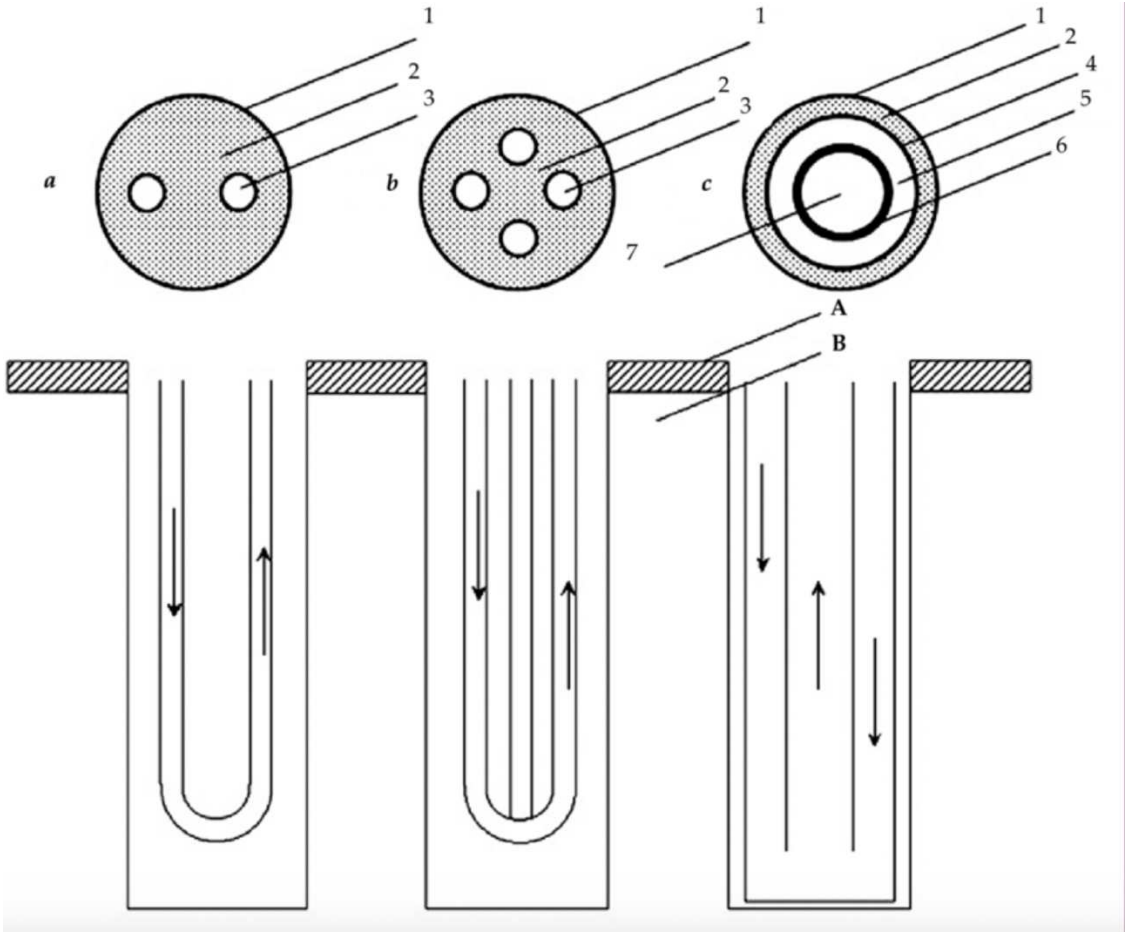

Figure 1. 2 ***Cross-sectional and side-view schematics of the main vertical closed-loop borehole heat exchanger configurations [5]***

Different configurations of vertical closed-loop borehole heat exchangers are shown in the figure 1.1, including:

(a) Single U-tube,

(b) Double U-tube,

(c) Coaxial (CBHE).

1.2.4 Technical Challenges and Research Needs

Despite their advantages, CBHEs face several technical challenges. One key issue is thermal short-circuiting, where heat from the ascending warm fluid is unintentionally transferred to the cooler descending fluid, reducing the system's overall efficiency. To mitigate this, careful selection of pipe materials and optimization of inner and outer pipe dimensions is essential. Additionally, parameters such as flow rate, fluid temperature, and borehole configuration must be fine-tuned to enhance thermal performance and long-term system reliability.

1.3 Literature Review

1.3.1 Thermal Performance of Coaxial Borehole Heat Exchangers

Coaxial geothermal heat exchangers (GHEs) have demonstrated equal or superior thermal performance compared to traditional single or double U-tube configurations. This advantage largely stems from the coaxial design's ability to circulate a larger fluid volume within the same borehole diameter, resulting in enhanced heat absorption or rejection for a given temperature change.

Raymond [6] showed that using a coaxial configuration with a thermally enhanced outer pipe reduced the required borehole length by up to 23% compared to U-tubes, due to lower borehole thermal resistance and increased fluid heat capacity. A long-term simulation by Quaggiotto [7] also found that an 80 m coaxial probe outperformed a double U-tube under realistic intermittent heat pump conditions.

Experimental studies confirm this trend. Wood [8] demonstrated that U-tube systems reached transitional-turbulent flow at lower flow rates, while coaxial probes remained laminar over the tested range yet still achieved similar heat transfer due to their geometry. Moreover, coaxial systems often use steel or other high-conductivity materials for the outer pipe, enhancing ground heat exchange compared to standard polyethylene U-tubes.

One key performance benefit lies in the reduction of thermal resistance between the fluid and ground. Acuña and Palm [9] reported that a coaxial pipe-in-pipe BHE had an effective borehole thermal resistance of about 0.03 K·m/W roughly half that of a typical U-tube. This makes coaxial systems particularly suitable for shallow-depth applications (e.g., ~80 m), where ground temperatures remain stable year-round.

Furthermore, coaxial systems can be more cost-effective to install. For example, Raymond *et al.* reported that CBHEs with thermally enhanced outer pipes can reduce required borehole length by up to 23%, leading to significant savings on drilling and installation costs [10]. This cost benefit is especially relevant in shallow, urban settings where drilling operations are a major expense.

In summary, literature indicates that a well-designed coaxial heat exchanger can outperform or at least match conventional designs in extracting geothermal heat, especially when its design is optimized for the specific ground conditions and load profile.

1.3.2 Influence of Pipe Geometry and Materials on Performance

1.3.2.1 Inner vs Outer Diameter:

The diameters of the inner and outer pipes play a crucial role in determining the flow distribution and heat transfer efficiency in coaxial heat exchangers. Unlike U-tube systems (where both legs have equal diameters), coaxial designs allow variation between inner and outer pipe sizes. This affects the cross-sectional areas of the inner channel and outer annulus, which in turn influences fluid velocities and convective heat transfer coefficients.

A larger inner diameter (i.e., a higher inner-to-outer diameter ratio) reduces the annular cross-sectional area, thereby increasing the velocity in the outer annulus and improving convective heat transfer at the borehole wall. However, it also reduces velocity inside the inner pipe, which may limit internal thermal short-circuiting between upward and downward flows. Conversely, a smaller inner diameter increases the annular area, reducing annular velocity and convective performance, but increases inner pipe velocity, potentially enhancing internal thermal mixing.

There is thus a trade-off in selecting the optimal diameter ratio to maximize heat transfer while minimizing pressure losses and pumping requirements. Parametric studies suggest that the ideal inner-to-outer diameter ratio for water-based systems lies between 0.60 and 0.70. For instance, Rafee [11] reported minimized pumping power at a ratio of 0.65, while Morchio and Fossa [12] found that ~0.60 offered the lowest thermal resistance in deep coaxial systems. Yekoladio [13] confirmed this optimal range, noting it may shift slightly based on flow regime and site-specific temperature conditions. In summary, selecting inner pipe sizes equal to 60–70% of the outer diameter is recommended. Ratios below 0.6 often cause excessive internal heat shunt, while ratios above 0.7 lead to high pumping costs with diminishing thermal benefit.

1.3.2.2 Pipe Material and Thermal Conductivity:

The pipe material particularly that of the outer pipe also significantly impacts system efficiency. Using high thermal conductivity materials such as steel or thermally enhanced HDPE reduces the borehole's thermal resistance and enhances heat exchange with the surrounding soil. Experimental data support this: Oh [14], showed that a coaxial BHE with a stainless-steel outer pipe achieved higher heat transfer performance compared to one using HDPE under identical conditions. Overall, proper selection of both geometry and material is essential for maximizing coaxial system performance.

The enhanced performance of coaxial systems using steel is largely attributed to steel's high thermal conductivity orders of magnitude greater than that of plastic. This allows for rapid and efficient heat transfer from the circulating fluid through the pipe wall into the surrounding ground. In contrast, the inner pipe is typically constructed from materials such as polyethylene or steel with added insulation, as its role primarily concerns minimizing internal heat shunting rather than facilitating ground heat exchange.

1.3.2.3 Inner Pipe Insulation:

To reduce thermal short-circuiting between upward and downward fluid streams, insulating the inner pipe especially in the upper borehole section where temperature gradients are largest—has been investigated. This insulation prevents heat from the rising warm fluid from transferring to the descending cold fluid, thus improving thermal efficiency. Zarrella [15] designed a coaxial BHE with a closed cell insulated inner pipe and added helical fins on the outer pipe to enhance heat exchange. Acuña and Palm [9] tested coaxial prototypes with and without partial inner pipe insulation and found little difference in performance for shallow depths, particularly when flow rates were optimized. However, in deeper boreholes or in systems operating over long durations, inner pipe insulation becomes more critical. It helps preserve thermal efficiency by minimizing shunt losses. Li [16] further demonstrated that shorter uninsulated segments (i.e., greater insulation coverage) led to modest gains in heat extraction per meter, validating the potential benefits of inner pipe insulation despite increased construction complexity.

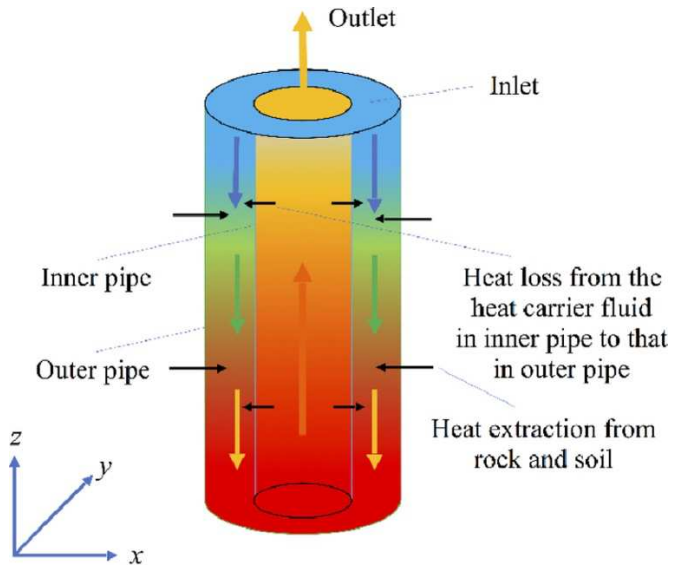

Figure 1. 3 ***Schematic of Thermal Short-Circuiting in a Coaxial Borehole Heat Exchanger (CBHE)***

1.3.2.4 Modelling and Simulation Tools for Coaxial GHEs

Modelling the thermal behaviour of coaxial borehole heat exchangers (GHEs) is critical for evaluating system performance and optimizing design. Over the years, researchers have developed a wide range of simulation approaches, including analytical models, semi-analytical solutions, full 3D numerical simulations, and building energy performance tools. These methods differ in complexity, computational requirements, and the level of physical detail they capture. Early foundational work by Oliver and Braud [17] introduced closed-form solutions for steady-state thermal performance of coaxial BHEs, extending classic line-source theory to account for concentric geometries. These models provided a simplified yet insightful way to estimate heat transfer performance without requiring intensive computation. In more recent work, Pan [18] proposed a new analytical model that improved the representation of transient behaviour in coaxial systems, offering better accuracy for time-dependent simulations and practical applications.

2

Fundamentals of Fluid and Thermal Processes

To accurately simulate and design coaxial geothermal heat exchangers, it is crucial to understand the underlying principles of fluid flow and thermal transport. This chapter introduces the core theoretical models that govern these phenomena, with emphasis on conservation laws and their relevance in numerical modelling for geothermal applications.

2.1 Governing Principles of Flow and Energy Transport

In fluid-based thermal energy systems, the working fluid behaviour is governed by fundamental conservation laws:

Mass conservation: Ensures that fluid does not accumulate or disappear within a system.

Momentum conservation: Accounts for the influence of both internal forces (e.g., viscosity) and external forces (e.g., pressure gradients, gravity).

Energy conservation: Describes how energy is transferred and transformed via convection, conduction, and mechanical work.

These laws are typically formulated through partial differential equations, which provide the foundation for computational fluid dynamics (CFD) and thermal simulations.

2.1.1 Fluid Transport in Confined Systems

To satisfy mass conservation, the net accumulation of fluid mass within a control volume must equal the difference between inflow and outflow. This relationship is mathematically expressed as:

$$\partial\rho/\partial t + \nabla \cdot (\rho\vec{v}) = 0 \qquad (2\text{-}1)$$

Here, ρ is the fluid density.

$\vec{v}$ is the fluid velocity vector

$\nabla \cdot (\rho\vec{v})$ represents the divergence of mass flux

2.1.2 Momentum Conservation (Fluid Motion)

To understand how fluids move under the influence of pressure and body forces (like gravity), the momentum equation is used. This is a general form of Newton's second law for fluids:

$$\partial(\rho\vec{v})/\partial t + \nabla \cdot (\rho\vec{v}\vec{v}) = -\nabla p + \nabla \cdot \tau + \rho\vec{\mathbf{F}} \qquad (2\text{-}2)$$

Where:

p: pressure

τ: viscous stress tensor

$\vec{\mathbf{F}}$: body force per unit mass (e.g., gravity)

This equation describes how pressure, viscosity, and external forces affect the motion of the fluid.

2.1.3 Energy Conservation (First Law of Thermodynamics)

The energy equation tracks how thermal and mechanical energy change within the fluid. It takes the form:

$$\partial/\partial t\,[\,\rho\,(e + \tfrac{1}{2}\,v^2)] + \nabla \cdot [\,\rho v\,(e + \tfrac{1}{2}\,v^2)] = -\nabla \cdot q + \nabla \cdot (\sigma \cdot v) + \rho v \cdot F \qquad (2\text{-}3)$$

Where:

e: internal energy per unit mass

$\vec{\boldsymbol{q}}$: heat flux vector

F: body force per unit mass

v^2: square of the velocity magnitude

This equation includes conduction, convection, work by viscous forces, and external energy input.

2.2 Flow Development and Boundary Layer Formation in Circular Channels

In closed-loop geothermal systems such as coaxial borehole heat exchangers, the internal fluid flow occurs through circular and annular geometries. Understanding how velocity profiles form and evolve is crucial, particularly because this directly affects convective heat transfer and pressure losses.

When a fluid begins to flow through a pipe, the velocity is typically uniform at the inlet. However, due to viscosity, the fluid layers adjacent to the wall experience drag, slowing them down. As a result, a velocity gradient starts to form from the wall toward the centreline. This process leads to the development of a boundary layer, which thickens along the pipe length until the profile reaches a steady, fully developed state (Figure 4.5).

The relationship between viscous forces and inertial forces in the fluid is captured by the Reynolds number:

$$\mathrm{Re} = \frac{V.L}{v} \qquad (2\text{-}4)$$

Where:

V: characteristic velocity of the fluid
L: characteristic length (often pipe diameter)
v: Kinematic viscosity

The Reynolds number determines the flow regime:

Laminar flow occurs at lower Re values.

Turbulent flow dominates at higher values.

For most geothermal systems with forced flow, turbulence is present, making accurate prediction of boundary layer behaviour especially important. The region adjacent to the wall, where velocity gradients are most intense, is responsible for most of the shear stress and heat exchange with the pipe surface. This area is often divided into sub-layers:

Viscous sublayer (near the wall, dominated by molecular diffusion)

Buffer layer

Log-law region (fully turbulent)

The geometry of coaxial pipes creates a similar boundary layer structure both in the annular injection path and in the central upward return pipe. The transition from entrance region to fully developed flow affects both thermal performance and frictional pressure drop, making it essential to account for in simulations and design. In the case of CBHEs, the annular space typically presents asymmetric boundary conditions, leading to non-uniform velocity distributions and complex thermal interactions that must be modelled using CFD or empirical correlations.

2.3 Pressure Losses and Friction Factors in Borehole Flow

In geothermal systems where fluid circulates through long, narrow channels such as in coaxial or annular borehole heat exchangers, the energy required to maintain flow is largely determined by frictional resistance. This resistance results in a pressure drop, which must be overcome by the pumping system, and therefore directly influences the required pump power and the system's operational efficiency.

2.3.1 Quantifying Friction in Pipe Flow

As fluid flows through a conduit, it interacts with the pipe walls, creating shear forces that slow the fluid and cause energy loss. These losses are described using a dimensionless parameter called the friction factor. Two widely used definitions exist:

Darcy friction factor (f_D) common in mechanical engineering

Fanning friction factor (f_F), used more in chemical engineering

Their relationship is:

$f_D = 4\, f_F$ (2-5)

The appropriate friction factor depends on the flow regime, which is determined by the Reynolds number. For laminar flow (Re < 2300), the resistance is well-defined and predictable. In contrast, turbulent flow (Re > 2300) requires empirical correlations due to its complexity.

2.3.2 Friction Factor Correlations

To estimate the Darcy friction factor under different flow conditions, standard formulas are applied:

For laminar flow:

$f_D = \frac{64}{Re}$ (2-6)

For turbulent or transitional flow, one commonly used model is the Gnielinski correlation, which provides a more accurate fit over a wide range of conditions:

$$f_D = \frac{1}{(0.79.ln(Re)-1.64)^2} \qquad (2\text{-}7)$$

These expressions allow for pressure drop calculations in systems such as borehole heat exchangers, where long pipe lengths amplify the cumulative effect of friction.

2.3.3 Practical Implications for CBHE Design

In coaxial systems, both the inner pipe and annular channel can be modelled as circular ducts, for which these correlations are directly applicable. Accurately calculating pressure losses ensures that the pumping system is correctly sized and avoids overspending energy to maintain circulation.

Moreover, since the pressure drop is proportional to the square of flow velocity, optimizing the flow rate becomes a key part of system design balancing thermal performance with mechanical efficiency.

2.4 Estimating Pressure Drop

In geothermal applications involving coaxial or annular pipe configurations, such as borehole heat exchangers, fluid experiences resistance as it moves along the inner surfaces of the system. This resistance results in a pressure drop, which must be overcome by the pump to maintain continuous flow.

2.4.1 Pressure Loss Modelling

The Darcy–Weisbach equation is commonly used to evaluate frictional pressure losses in internal flows:

$$\Delta p_f = f_d . \frac{L}{D_h} . \rho \frac{V^2}{2} \qquad (2\text{-}8)$$

Where:

Δp_f : pressure loss due to friction

f_d : Darcy friction factor

L: pipe or flow length

Dh: hydraulic diameter

ρ: Fluid density

V: average velocity of the fluid

For circular conduits, Dh corresponds to the pipe diameter. In annular configurations, such as those found in CBHE systems, the hydraulic diameter is calculated as the difference between outer and inner pipe diameters.

2.5 Computational Fluid Dynamics (CFD)

Computational Fluid Dynamics (CFD**)** is a powerful tool used to analyse complex thermal and hydraulic behaviour in engineered systems. It enables the numerical solution of the conservation equations of mass, momentum, and energy in fluid domains.

CFD simulations typically consist of three stages:

1. Pre-processing: definition of geometry, mesh generation, material properties, and boundary conditions
2. Solver: numerical integration of the governing equations using discretization methods (e.g., Finite Volume Method or Finite Element Method)
3. Post-processing: visualization of results, data extraction, and performance evaluation

2.5.1 CFD in Geothermal Modelling

In the context of borehole heat exchangers, CFD helps capture:

- Transient thermal behaviour over time
- Boundary layer development near pipe walls
- Effects of turbulence on heat transfer
- Thermal resistance across solid-fluid interfaces

Mesh quality, convergence criteria, and appropriate turbulence models (e.g., k–ε or SST) are crucial to ensure the reliability of results.

2.5.2 Numerical Considerations in CFD Modelling

To reliably simulate fluid flow and heat transfer within geothermal systems, a carefully constructed computational model is essential. This includes a mesh that accurately represents the geometry and a solver setup that balances precision with efficiency.

2.5.3 Mesh Design and Domain Discretization

In CFD, the physical geometry is divided into a finite set of small subdomains (or cells), which form the computational mesh. Depending on the complexity and dimensionality of the geometry, different element types are used:

- 2D models often employ triangular or quadrilateral elements.
- 3D models may include tetrahedrons, pyramids, or hexahedrons.

The choice of mesh topology, element size, and refinement strategy depends heavily on:

- The geometry of the domain
- The type of physics being modelled (e.g., turbulence, conduction)
- The available computational resources

Mesh quality is critical. Characteristics like skewness, aspect ratio, and orthogonality must be within acceptable limits to ensure numerical accuracy and solver stability. However, using excessively fine meshes may increase simulation time without improving accuracy significantly. Therefore, a balance between resolution and efficiency must be maintained.

2.5.4 Mesh Independence and Convergence

To ensure that simulation results are not biased by mesh size, mesh independence studies are conducted. This involves comparing results from simulations using progressively refined meshes. If key outputs (e.g., outlet temperature) remain stable as the mesh is refined, the solution is considered mesh independent. Only after confirming mesh independence should simulation results be considered reliable for performance evaluation or design comparison.

2.5.5 Modelling Turbulence in Engineering Flows

In geothermal systems like CBHEs, the working fluid often operates in a turbulent regime, especially at higher flow rates. Turbulence is characterized by chaotic eddies and fluctuations that are too computationally expensive to resolve directly (as in Direct Numerical Simulation). Therefore, turbulence is usually modelled using Reynolds-Averaged Navier–Stokes (RANS) equations, which solve for mean flow variables and model the effects of turbulence through additional equations.

2.5.5.1 Turbulence Model Options

Several models are available depending on the application:

- The mixing length model is one of the earliest approaches, suitable for simple, steady shear flows. While computationally light, it lacks accuracy for complex geometries or recirculating flows.
- The Spalart Allmaras model is more advanced and widely used in aerodynamic simulations. It solves a single transport equation and is effective for boundary-layer-dominated flows. However, it may be less reliable for internal flows with strong separation or swirl.

The Spalart Allmaras model is more advanced and widely used in aerodynamic simulations. It solves a single transport equation and is effective for boundary-layer-dominated flows. However, it may be less reliable for internal flows with strong separation or swirl.

For CBHE applications, where near-wall behaviour and convective transport dominate heat transfer, more sophisticated models like k–ε or SST k–ω are often more appropriate (discussed in the next section).

2.5.5.2 Turbulence Modelling in CFD Simulations

Modelling turbulence accurately is essential for simulating internal flow behaviour in geothermal systems, especially when flow regimes are far from laminar. Several models are available, each balancing complexity with computational cost and accuracy.

k–ε Turbulence Model:

The k–ε model is among the most widely adopted in engineering applications due to its simplicity and robustness. It requires the solution of two transport equations: one for the turbulent kinetic energy (k) and another for its dissipation rate (ε). It performs well in fully turbulent flows and is suitable for a broad range of industrial geometries.

However, its limitations become apparent near walls and in flows with separation, curvature, or swirling motion, where turbulence behaviour becomes more complex.

k–ω and SST Models:

An alternative to the k–ε model is the k–ω turbulence model, which replaces the dissipation rate equation with one for the specific dissipation rate (ω). This approach provides better resolution in near-wall regions but can be more sensitive to freestream values.

The SST (Shear Stress Transport) model merges the strengths of both approaches. It uses the k–ω formulation near the wall to capture steep gradients and switches to k–ε in the outer flow to maintain stability. This hybrid model is particularly useful for internal pipe flows such as those in coaxial boreholes where heat exchange near the wall is crucial.

Since detailed resolution of the boundary layer requires very fine meshes and high computational cost, many CFD packages offer wall functions. These are semi-empirical models that approximate velocity and temperature gradients near the wall without resolving every sublayer directly.

By combining turbulence models with appropriate wall functions, simulations can capture key boundary layer effects while keeping computational demands reasonable a valuable strategy in simulating long CBHE domains.

2.6 Heat Transfer Principles

In coaxial geothermal systems, the transport of thermal energy between the fluid and surrounding materials occurs through two primary mechanisms: conduction through solids and convection within the fluid. This section introduces the fundamental laws that describe heat movement and are used to evaluate thermal performance.

2.6.1 Conduction

Conduction is the process by which heat is transferred through a solid or stationary medium due to a temperature gradient. In CBHEs, conduction occurs through pipe walls, insulation, grout, and the surrounding soil.

The general energy balance for conduction (based on the first law of thermodynamics) is:

$$\rho C_p \frac{\partial T}{\partial t} + \rho C_p \vec{v}.\nabla T = -\nabla.\vec{q} + \beta T\left(\frac{\partial p}{\partial t} + \vec{v}.\nabla_p\right) + \vec{\tau}:\nabla\vec{v} + Q \qquad (2\text{-}9)$$

Where:

ρ: density
T: Temperature
$\vec{v}$: fluid velocity
$\vec{q}$: conductive heat flux
$\vec{\tau}:\nabla\vec{v}$: viscous dissipation
Q: internal heat source
β: volumetric thermal expansion coefficient
P: Pressure

Conduction is the transfer of thermal energy due to a temperature gradient within a stationary medium. In pipe walls, grout layers, and surrounding geological formations, heat is conducted from hotter regions to cooler ones following Fourier's law:

$$\dot{q}_x = -kA\frac{dT}{dx} \qquad (2\text{-}10)$$

Where:

$\dot{q}_x$: rate of heat transfer in the x-direction

k: thermal conductivity of the material

A: Cross-sectional area perpendicular to flow

$\frac{dT}{dx}$: Temperature gradient

2.6.2 Forced Convection

Forced convection involves heat transport through a fluid as it is pushed or circulated by external forces, such as pumps. In coaxial geothermal systems, this mechanism dominates inside the working fluid, where flow velocity significantly enhances heat transfer between the fluid and pipe wall.

According to Prandtl's boundary layer theory, a thin thermal region forms near solid surfaces where temperature changes rapidly. By applying Fourier's law across this boundary layer, the convective heat transfer rate can be approximated as:

$$\dot{q} = -KA\frac{T_{fluid}-T_{surface}}{\delta_t} \quad (2\text{-}11)$$

Where:

δ_t: $thermal\ boundary\ layer\ thickness$

T_{fluid} : fluid temperature

$T_{Surface}$: pipe wall temperature

2.6.2.1 Convective Heat Transfer Parameters

In forced convection, heat exchange between a solid boundary (e.g., pipe wall) and a moving fluid depends on both the fluid's motion and its thermophysical properties. This interaction is quantified using the convective heat transfer coefficient, h, which links the local temperature difference to the rate of heat flow.

2.6.2.2 Convective Heat Transfer Rate and Resistance

When heat is transferred across the boundary layer separating the fluid and the wall, the rate is expressed as:

$$\dot{q} = hA(T_{fluid} - T_{surface}) \quad (2\text{-}12)$$

Using boundary layer thickness δ_t, the coefficient h can be estimated from:

$$h = \frac{k}{\delta_t} \quad (2\text{-}13)$$

And the heat transfer rate becomes:

$$\dot{q} = -\frac{k}{\delta_t} A(T_{fluid} - T_{surface}) \quad (2\text{-}14)$$

Just as in conduction, a thermal resistance analogy can be applied for convection:

$$R_{conv} = \frac{1}{hA} \quad (2\text{-}15)$$

This form simplifies system-level analysis of heat exchange across solid-fluid interfaces.

2.6.2.3 Nusselt Number

The Nusselt number (Nu) is a dimensionless parameter that characterizes the ratio of convective to conductive heat transfer at a boundary:

$$Nu = \frac{hL}{k} \quad (2\text{-}16)$$

Where:

L: characteristic length (typically pipe diameter)

k: thermal conductivity of the fluid

A Nusselt number of 1 indicates pure conduction. Higher values signal enhanced convection.

In geothermal systems, turbulent flow significantly increases the Nusselt number, improving the rate at which heat is exchanged between the fluid and surrounding materials (pipe wall, grout, or soil).

3

Methodology

This chapter outlines the numerical methodology employed to evaluate and optimize the thermal performance of a coaxial borehole heat exchanger (CBHE) through simulation. It describes the COMSOL Multiphysics® modelling setup, the geometric variations tested, and the real-world application of the optimal configuration using Termus and Geotermus software.

3.1 Overview

A series of simulations were performed in COMSOL Multiphysics® to investigate the effect of pipe diameter variations on the thermal performance of a CBHE. A 2D axisymmetric model was developed, varying both inner and outer pipe diameters, to assess their impact on the outlet fluid temperature, which serves as a key performance indicator.

All environmental and operating conditions such as inlet temperature, flow rate, and soil properties were kept constant. The aim was to identify the geometric configuration that delivers the highest thermal output under identical boundary conditions.

Based on the most effective pipe configuration obtained from the simulations, the design was tested in a real-world scenario. Using Termus and Geotermus, the selected configuration was used to simulate the heating demand of a residential building consisting of four individual housing units. The goal was to estimate the required drilling depth needed to meet the total energy demand using the optimized CBHE setup.

3.2 Project description and design

3.2.1 Baseline Simulation Case

The baseline simulation modelled in COMSOL represents a standard coaxial borehole heat exchanger configuration. In this setup, the working fluid enters the borehole through the annular space between two vertically aligned concentric pipes and returns to the surface via the inner pipe. Heat is absorbed from the surrounding ground through the outer pipe wall by conduction and transferred to the circulating fluid (Figure1.2).

The simulation domain includes both solid components (pipes and surrounding soil) and fluid regions. Heat transfer was modelled as conduction within the solid parts and convection within the fluid zones.

To evaluate the impact of geometry on thermal performance, various combinations of inner and outer pipe diameters were tested. The baseline case thus serves as a reference framework against which the performance of other configurations is compared.

3.2.2 Geometric Influence Evaluation

This baseline model provides the foundation for analysing how pipe geometry affects system efficiency. With all other parameters such as material properties, soil conditions, and boundary settings kept constant, the pipe diameters were systematically varied to assess their influence on outlet fluid temperature, a key indicator of performance. After identifying the optimal geometry through simulation, it was applied in a practical space heating and cooling scenario using Termus and Geotermus. This integration enabled the estimation of the required borehole depth to satisfy the heating demand of a modelled residential apartment building composed of four housing units.

3.2.3 Borehole and Fluid Flow Conditions

The modelled CBHE consists of two concentric pipes vertically placed in the borehole. Water enters through the annular gap between the pipes; exchanges heat with the surrounding soil and returns via the inner pipe. The system reflects the climatic and geological conditions of Padova, Italy, where the average annual ground surface temperature is 13 °C [19] and the subsurface temperature at 85 m depth is 15.4 °C [20].

Initially, a constant flow rate of 12 L/min was used in all simulations to analyse the impact of different inner and outer pipe geometries on thermal performance. After identifying the best-performing configuration based on outlet temperature, additional simulations were carried out using different flow rates (9, 12, and 15 L/min) to evaluate the effect of flow rate variation on system performance. The inner pipe length is set to 79 m, the outer pipe extends to 80 m, and the total drilling depth is fixed at 85 m. All other thermal and physical parameters were kept constant across the simulations. The properties of the fluid, pipes, ground, and concrete are summarized in Table 3.1.

3.2.4 COMSOL Modelling Approach

To evaluate the thermal performance of coaxial borehole heat exchangers (CBHEs), a numerical model was developed using COMSOL Multiphysics® version 6.2. The simulations were carried out in a 2D axisymmetric domain, which allowed for efficient yet accurate representation of the physical system by taking advantage of the borehole's radial symmetry. The aim was to analyse how pipe geometry and flow rate influence heat exchange under realistic ground conditions representative of Padova, Italy.

The full borehole depth of 85 meters was included in the model, with the inner and outer pipes each extending to 80 meters. The remaining 5 meters at the bottom were modelled as ground only, reflecting real installation conditions and avoiding artificial boundary effects at the pipe ends. Unlike in simplified models, pipe wall thicknesses were included, based on commercial product

specifications for each tested pipe diameter, allowing for a more realistic evaluation of conductive resistance through the pipe walls.

All thermal and physical properties of materials (fluid, pipes, soil, and concrete) were treated as constant. Ground temperature conditions were set according to local climatic data: 13 °C at the surface and 15.4 °C at 85 m depth, reflecting the typical geothermal gradient of the region. The working fluid was water, assumed incompressible with constant thermophysical properties at 15 °C.

Simulations were performed under two operating scenarios:

Heating mode: a constant inlet temperature of 5 °C was imposed, and three flow rates (9, 12, and 15 L/min) were tested.

Cooling mode: an inlet temperature of 20 °C was used with a fixed flow rate of 12 L/min.

These simulations allowed evaluation of how flow conditions and pipe geometries affect outlet temperature and heat transfer rate. To enhance result reliability, a coupled modelling strategy was adopted, combining a steady-state step with a time-dependent step. The steady-state analysis established the velocity field in the fluid domain, while the time-dependent study captured the system's unsteady heat transfer behaviour. This approach ensured realistic and dynamic predictions of system performance over time.

Finally, the model was validated using real operational data provided by RED SRL, the internship host company. The data originated from one of their completed geothermal projects located in Putte Belgium, where a coaxial borehole heat exchanger system had been monitored for one season. The simulated temperature profiles closely matched the measured values, confirming the accuracy and applicability of the numerical model for predicting system performance and supporting its use in future design analyses.

3.2.4.1 Thermal-Fluid Physics and Turbulence approach

The physical model developed in this study integrates the Heat Transfer in Solids and Fluids, Turbulent Flow, and Non isothermal Flow modules to simulate the thermal and fluid dynamics of the coaxial borehole heat exchanger (CBHE). Based on the calculated Reynolds numbers along the flow path, turbulence modelling was essential to accurately capture the transition between laminar and turbulent regimes.

To achieve this, the k-ω turbulence model was selected due to its strong performance in resolving near-wall flows and capturing sharp velocity gradients. This is particularly important in the lower section of the borehole, where the fluid path makes a 180° turn before entering the inner pipe, introducing significant curvature and shear effects. The model enables reliable prediction of heat transfer and pressure losses under such conditions. Additionally, wall functions were employed to

simplify the treatment of near-wall regions by approximating the velocity profile without the need to fully resolve the boundary layer.

3.2.4.2 Study Type and Simulation Strategy

The simulation approach combines a stationary study and a time-dependent study to capture both steady-state and transient system behaviour. The stationary step is initially used to solve for velocity and pressure fields within the fluid domain, ensuring a stable flow regime. These results are then passed as initial conditions to the time-dependent study, which models the system's thermal response over time. This combined strategy enables a more realistic representation of heat transfer dynamics within the borehole heat exchanger, especially under changing operational conditions.

3.2.4.3 Geometry

The computational domain of the coaxial borehole heat exchanger (CBHE) was developed using a 2D axisymmetric configuration, providing a computationally efficient yet geometrically accurate representation of the real 3D cylindrical system. This approach simulates the system by rotating a 2D cross-section around the central vertical axis. The modelled geometry includes all critical layers: the inner pipe, the annular flow region, the outer pipe wall, the cement layer, and the surrounding ground.

The total vertical extent of the model is 85 meters, corresponding to the actual borehole depth. Both the inner and outer pipes are modelled as 80 meters long, matching the active heat exchange section. Additionally, the model incorporates a bottom flow reversal section that enables the injected fluid to reverse direction and flow upward through the inner pipe. This structural detail allows simulation of both the downward and upward flow within a single domain. A schematic of the modelled geometry is illustrated in Figure 3.1.

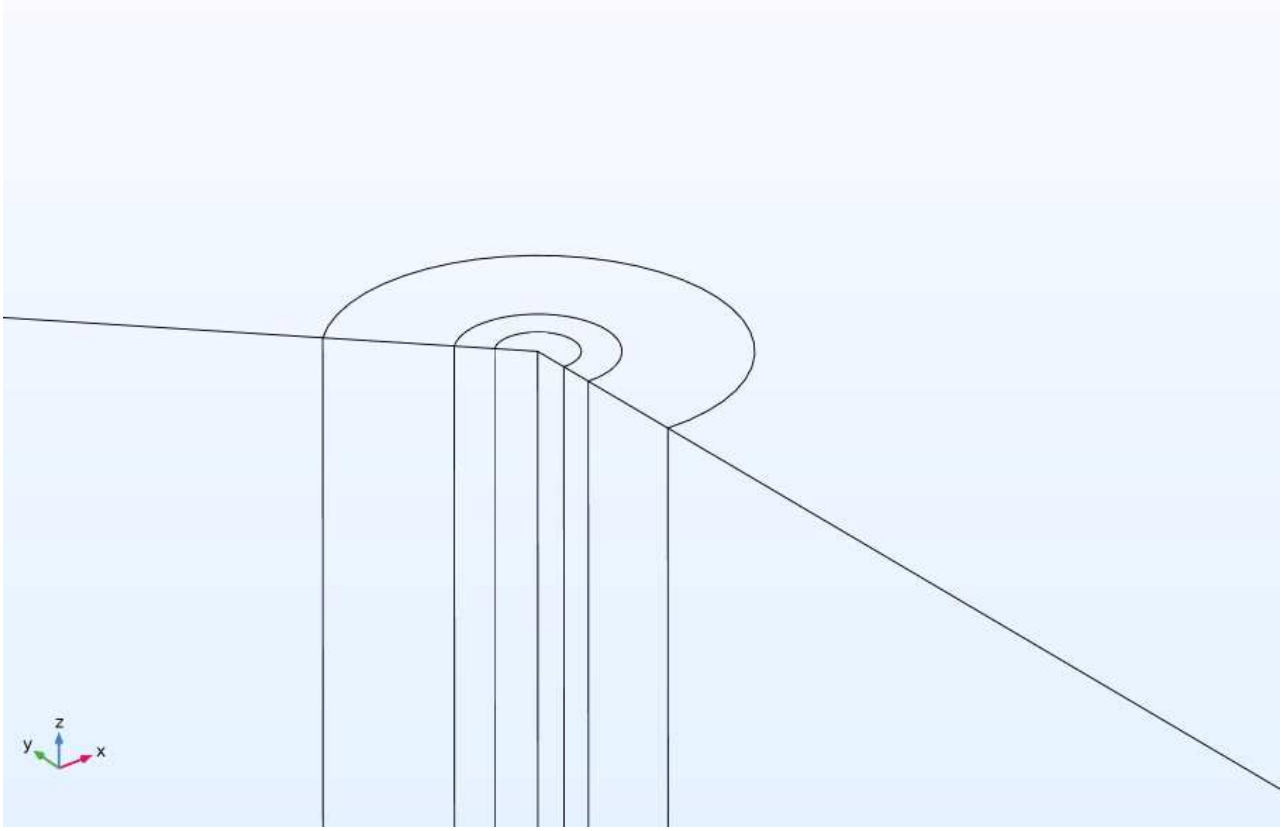

Figure 3. 1 **3D Slice View of the Axisymmetric Coaxial Borehole Heat Exchanger (CBHE) Geometry**

The concentric cylindrical regions represent different components of the system:

- The innermost circle corresponds to the inner pipe,
- The second ring represents the outer pipe,
- The third annular layer between the outer pipe and the soil is the cement-filled sealing zone,
- The outermost region is the surrounding ground domain.

In this model, the external pipe thickness was fully included, based on actual pipe specifications, to better represent the real thermal resistance. All layers of the system inner pipe, annular region, outer pipe, cement, and surrounding soil were modelled in detail. The mesh was refined near the pipe walls and fluid zones, where sharper temperature and velocity changes occur, and kept coarser in the outer ground.

3.2.4.4 Materials

This simulation involved five materials across the model's domains: water as the working fluid, PE100 for the inner pipe, S195T steel for the outer pipe, and standard cement and ground materials. For simplification and consistency with the overall simulation strategy, the thermal and physical properties of all materials were defined as constant, without dependence on temperature. Material properties were either selected from the COMSOL® built-in library or manually assigned based on trusted engineering data. The values used in the model are presented in Table 3.1 and include the most relevant thermal characteristics for each domain.

Domain	Parameter	Symbol	Value	Unit
Circulating fluid (water)	Density	ρ	1000	$\frac{kg}{m^3}$
	Specific heat capacity	C	4180	$\frac{J}{kg.K}$
	Thermal conuctivity	k	0.6	$\frac{W}{m.K}$
	Flow rate	$\dot{V}$	9 , 12, 15	$\frac{L}{min}$
Inner pipe (PE 100)	Density	ρ	950	$\frac{kg}{m^3}$
	Specific heat capacity	C	2200	$\frac{J}{kg.K}$
	Thermal conductivity	k	0.4	$\frac{W}{m.K}$
Outer pipe (S195T)	Density	ρ	7850	$\frac{kg}{m^3}$
	Specific heat capacity	C	470	$\frac{J}{kg.K}$
	Thermal heat conductivity	k	48	$\frac{W}{m.K}$
Grouting material (concrete)	Density	ρ	2300	$\frac{kg}{m^3}$
	Specific heat capacity	C	880	$\frac{J}{kg.K}$
	Thermal heat conductivity	k	1.8	$\frac{W}{m.K}$
Ground	Density	ρ	2600	$\frac{kg}{m^3}$
	Specific heat capacity	C	850	$\frac{J}{kg.K}$
	Thermal heat conductivity	k	2.9	$\frac{W}{m.K}$

Table 3. 1 ***Thermo-physical Properties of Materials and Fluids Used in the Simulation***

3.2.4.5 Thermal Boundary Conditions

In this model, boundary conditions were defined within the Heat Transfer in Solids and Fluids interface to represent both heating and cooling scenarios. A symmetry condition was applied along the central vertical axis of the coaxial geometry to take advantage of its rotational symmetry, allowing a simplified 2D axisymmetric setup.

For the heating mode, a fixed inlet temperature of 5 °C was applied to the circulating fluid. In the cooling mode, the inlet temperature was increased to 20 °C to reflect typical summer conditions. In both cases, the external ground environment was modelled with temperature constraints: a surface temperature of 13 °C, representing the average annual air temperature in Padova, and a bottom boundary temperature of 15.4 °C, consistent with the geothermal gradient at 85 m depth. These values refer to average conditions and may vary during the year depending on seasonal and operational factors. The 85 m depth refers to the full modeled domain, while the active length of the geothermal probe is 80 m.

All materials were treated as having constant thermophysical properties, and the water used as the heat transfer fluid was modelled as incompressible for numerical stability and simplicity.

Operating Mode	Domain	Boundary Parameter	Location	Value	Unit
Heating	Circulating fluid	Inlet Temperature	Inlet (annular side)	5	**°C**
	Ground	Surface Boundary	Surface (0m)	13	**°C**
		Bottom Boundary	Bottom (85m)	15.4	**°C**
Cooling	Circulating fluid	Inlet Temperature	Inlet (annular side)	20	**°C**
	Ground	Surface Boundary	Surface (0m)	13	**°C**
		Bottom Boundary	Bottom (85m)	15.4	**°C**

Table 3. 2 ***Temperature Boundary Conditions Applied in Heating and Cooling Scenarios***

3.2.4.6 Mesh

To simulate the coaxial borehole heat exchanger (CBHE), a mixed mesh approach was employed. The pipe domains (inner and outer) were discretized using a structured quadrilateral mesh, which provides high accuracy for aligned flow in cylindrical regions. This setup is ideal for resolving the heat and fluid dynamics along the vertical axis of the exchanger.

In contrast, triangular elements were assigned to the cement and surrounding ground, where flexibility in shape adaptation is more critical. These unstructured meshes accommodate the complex outer geometry without requiring a high level of local refinement.

To improve the resolution near the pipe walls, boundary layer elements were added to both the inner and outer pipe surfaces. This enhancement allows for better capture of velocity and thermal gradients, especially important when using the Low Reynolds number k-ε turbulence model.

The mesh configuration was developed using COMSOL®'s Fine mesh setting, which automatically adjusts element sizes based on geometric detail. Additional refinements were implemented at specific transitions to ensure stable and accurate results.

In total, the mesh consists of approximately 82,625 elements, comprising 25,340 triangular and 57,285 quadrilateral cells. The average element quality, based on the skewness metric, reached 0.9357, confirming that the mesh meets recommended standards for coupled heat transfer and turbulent flow problems. The total meshed area of the model is 255 m^2, and the minimum element quality observed was 0.0033, occurring near more complex junctions.

To numerically analyse the coaxial borehole heat exchanger (CBHE) system, a combination of structured and unstructured meshing strategies was applied. The goal was to ensure high simulation accuracy while keeping the model computationally efficient.

The fluid domains inside the inner and outer pipes were discretized using a structured quadrilateral mesh (Mapped), which is particularly suitable for axial flow. This structured configuration ensures better alignment with velocity and temperature gradients, providing highly regular and stable elements throughout the vertical pipe sections.

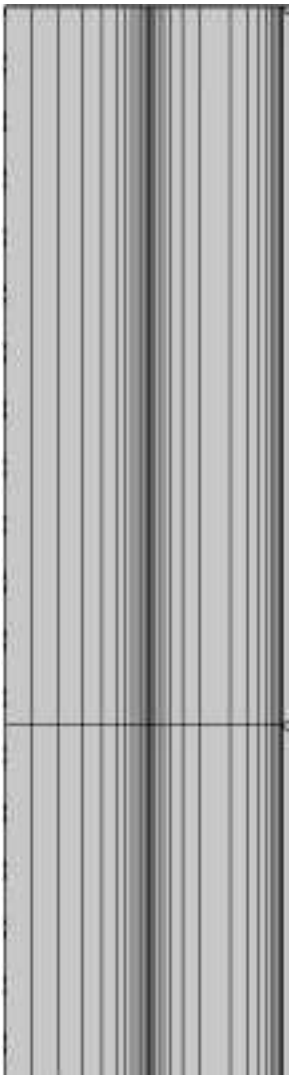

Figure 3. 2 ***Structured quadrilateral mesh applied to the inner and outer pipe domains***

For the cement and ground regions, a Free Triangular mesh was employed. This choice allows greater geometric flexibility and is better suited for capturing thermal gradients near the borehole wall, especially in radially distributed domains.

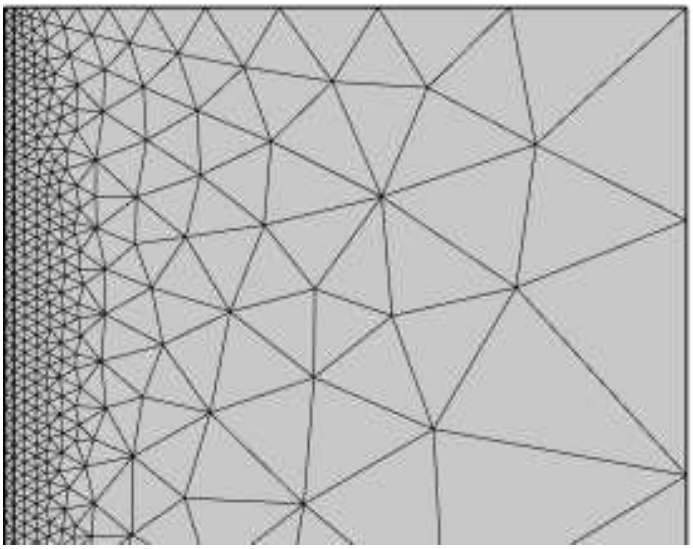

Figure 3. 3 ***Unstructured triangular mesh in the ground region, showing finer resolution near the borehole wall and coarser elements farther away***

Boundary layer meshes were included along the pipe walls to accurately capture the thermal and velocity gradients in near-wall regions. These layers are essential for low Reynolds number turbulence modelling, which requires additional resolution close to the surface.

3.2.4.6.1 Meshing Verification

To confirm the accuracy and consistency of the simulation results, a mesh independence study was conducted. This process ensures that the numerical outputs, such as outlet temperature and thermal performance, are not significantly affected by the size or distribution of the mesh.

In this project, two slightly different fine mesh configurations were tested. Despite the variations in the element distribution, both meshes produced nearly identical results. This indicates that the selected mesh is sufficiently refined and that the solution is independent of further mesh discretization. The overall mesh quality was also evaluated using the skewness metric in COMSOL. The average element quality was found to be 0.9357, which reflects a high level of regularity and reliability in the mesh structure. This confirms that the mesh is suitable for stable and accurate numerical simulation. Considering both the mesh quality and the results of the grid independence check, the chosen mesh setup was adopted for all further simulations in this study.

3.2.4.7 Validation

To ensure the accuracy of the developed 2D COMSOL® asymmetric model, a validation process was performed using real operational data from a monitored coaxial geothermal system located in Putte,

Belgium [21]. This field data served as a reference to compare and assess the numerical performance of the simulation. The validation focused on evaluating the temperature profiles at different depths over a specified period of operation. By comparing the simulated outlet temperatures and thermal behaviour against the actual measurements collected from the field over a full seasonal period, the model's capability to reproduce realistic system behaviour was confirmed. This comparison demonstrated strong agreement between the COMSOL simulation and the real data, supporting the model's reliability for further parametric and performance analysis under different configurations.

3.2.4.8 Parametric Simulation Strategy for Geometry and Flow Rate Optimization

To better understand how design changes impact the performance of the coaxial borehole system, a set of simulation scenarios were developed where key parameters were adjusted. These tests helped to highlight which configurations improve thermal efficiency under realistic operating conditions.

The first series of simulations focused on changing the dimensions of the pipes, specifically the diameters of both the inner and outer tubes. During these runs, the material of the pipes, the circulating fluid (water), and the flow rate (12 liters per minute) were kept unchanged. The goal of this stage was to observe how different pipe sizes influence the outlet temperature and the amount of heat exchanged with the surrounding soil, both in heating mode (inlet temperature: 5 °C) and cooling mode (inlet temperature: 20 °C).

Once the most efficient configuration was identified in terms of outlet thermal performance, a second set of simulations was performed using that same geometry. This time, the flow rate was the variable of interest. Simulations were carried out with three different flow rates: 9, 12, and 15 liters per minute, while keeping all other settings constant. This step allowed evaluating the impact of fluid velocity on system performance and confirming whether higher or lower flow rates contribute to improved thermal output.

Each test provided insight into how individual design decisions affect the overall behaviour of the geothermal exchanger, helping guide both technical optimization and practical application.

Inner pipe diameter (mm)	Inner pipe wall thickness (mm)	Outer pipe diameter (mm)	Outer pipe wall thickness (mm)	Model number	Length of the inner pipe(m)	Length of the outer pipe(m)
63	5,4	88,9	3,65	1	79	80
50	4,3	88,9	3,65	2	79	80
40	3,5	88,9	3,65	3	79	80
50	4,3	76,1	3,25	4	79	80
40	3,5	76,1	3,25	5	79	80
32	2,8	76,1	3,25	6	79	80
50	4,3	60,3	3,25	7	79	80
40	3,5	60,3	3,25	8	79	80
32	2,8	60,3	3,25	9	79	80
32	2,8	48,3	2,9	10	79	80
25	2,2	48,3	2,9	11	79	80

Table 3. 3 ***Coaxial heat exchanger models with different pipe dimensions and fixed pipe length.***

After identifying the most effective coaxial configuration through simulation (which will be shown in the results chapter), the study proceeded to evaluate its applicability in a real-world scenario. Using Termus and Geotermus software, the selected configuration was applied to a residential building with four residential units, to estimate the required borehole length needed to meet the energy demand for heating and cooling. This step helped bridge the simulation results with practical system design considerations.

3.2.5 Termus and Geotermus Setup for Building Energy Modelling

In this section, the methodology adopted to simulate the building's energy performance using the Termus and Geotermus software is described. After completing the COMSOL simulations and identifying the optimal coaxial heat exchanger configuration, the next phase involved evaluating the thermal behaviour of a real residential building located in Padova, constructed in the 1960s. The building includes four separate housing units distributed over multiple floors. Using Termus, the full 3D geometry was modelled, and thermal zones were defined for each apartment. Building components such as walls, roofs, and windows were assigned specific thermo-physical properties based on available data. Several insulation scenarios were also created to compare their effects on heating and cooling demand. The resulting monthly energy demands from Termus were then used as inputs in Geotermus.

The simulations performed in Termus were carried out in accordance with Italian national standards, particularly the UNI/TS 11300 series and UNI EN 15193:2008, as officially supported by the software's CTI certification[22]. The simulations performed in Geotermus were carried out in accordance with ASHRAE standards, as stated by the software developers[23].

This software allowed for climate-based sizing of geothermal systems, automatically applying Padova's environmental conditions. The coaxial borehole heat exchanger configuration from COMSOL, as well as the heat pump characteristics and working fluid (water), were implemented in Geotermus. The objective was to determine the number and depth of boreholes required for different thermal load scenarios, both for individual apartments and the entire building considered as a single system.

3.2.5.1 Building Geometry and Zone Definition in Termus

Figure 3. 4 ***Representation of the Modelled Residential Building in Termus***

Figure 3.4 shows the 3D architectural model of the residential building located in Padova, which was used as the base geometry for energy simulations. The structure includes a ground floor (not heated or cooled), two residential floors (each with two separate units), and a pitched roof (copertura). This model was developed to accurately define the geometry and envelope characteristics before importing it into Termus for thermal performance analysis.

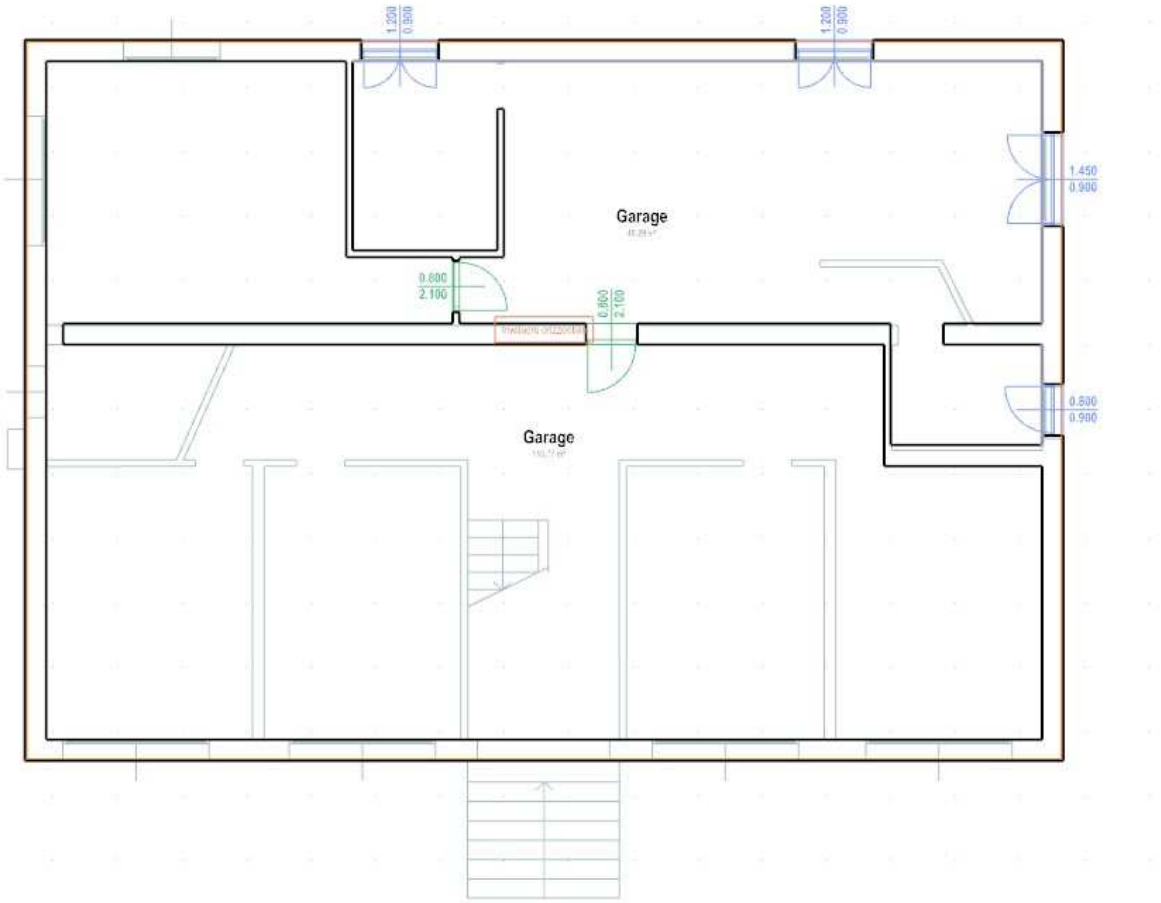

Figure 3. 5 ***Ground Floor Plan of the Modelled Residential Building***

Figure 3.5 illustrates the floor plan of the ground level of the residential building. This level is entirely allocated to garage space, featuring multiple parking areas and access points. The layout includes separate garage rooms and an internal staircase that connects the garage to the upper residential floors, ensuring functional vertical circulation within the building.

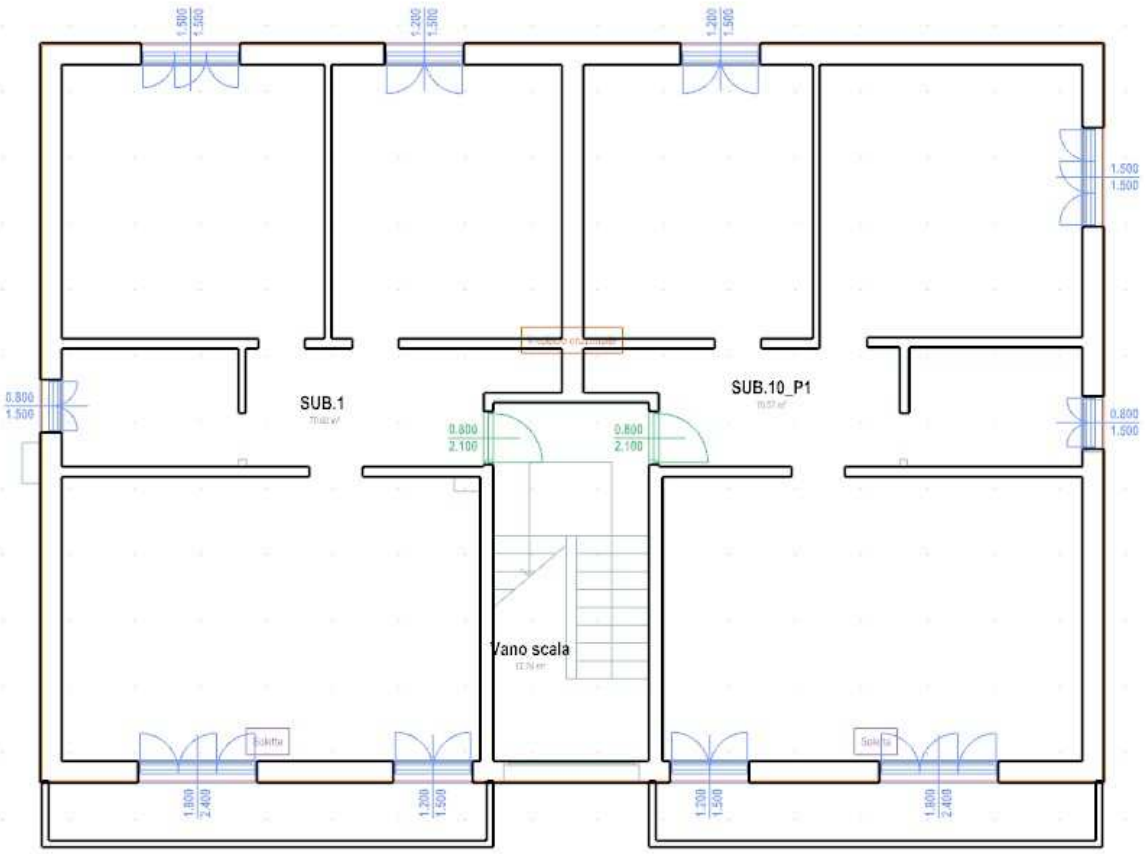

Figure 3. 6 ***First Floor Plan of the Residential Building (Two-Family Unit Layout)***

This image shows the floor plan of the first level of the residential building, which includes two distinct housing units: SUB.1 and SUB.10. The central staircase (Vano scala) connects this level to both the ground and upper floors. Each unit contains multiple rooms, with independent entrances and access to external balconies, reflecting a typical layout for a two-family floor arrangement.

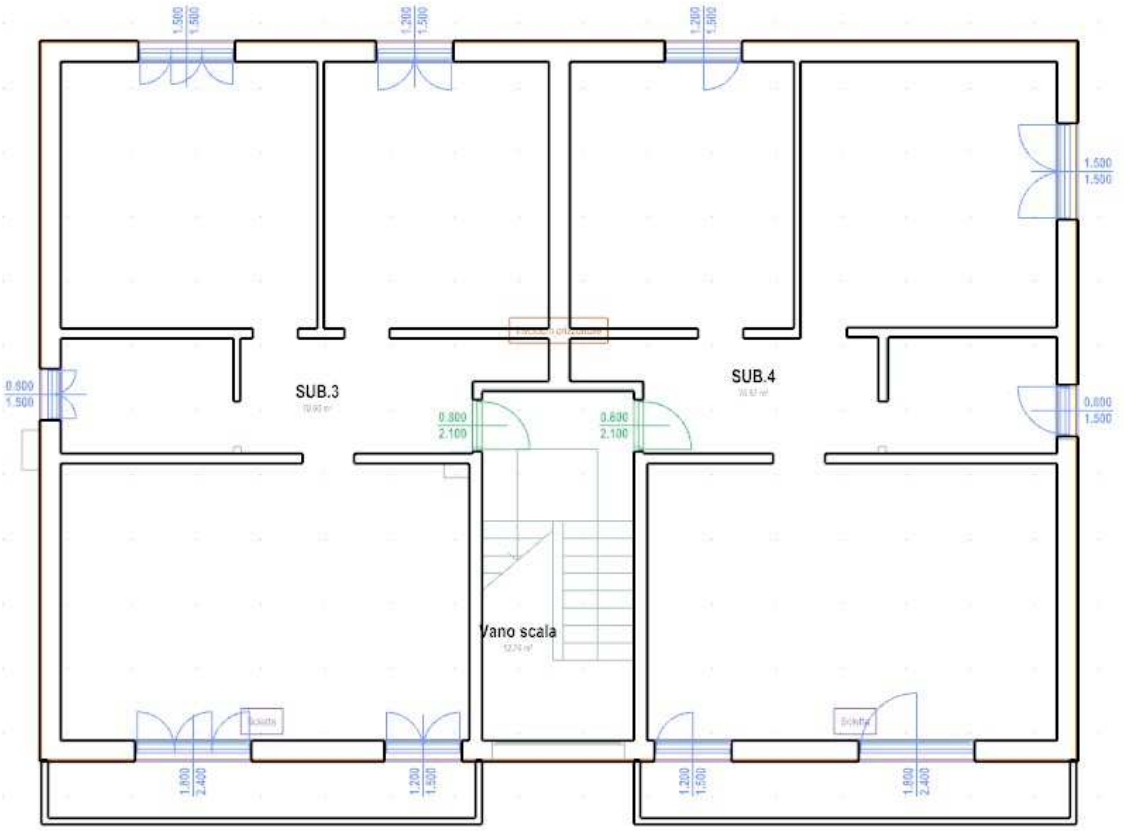

Figure 3. 7 ***Second Floor Plan of the Residential Building (Housing Units SUB.3 and SUB.4 with Central Staircase Access)***

This image illustrates the second-floor plan of the building, housing two residential units: SUB.3 and SUB.4. Like the first floor, access to these apartments is provided through the central staircase (Vano scala). Each unit is symmetrically laid out, offering multiple rooms and access points, and features external doors leading to balconies or outdoor spaces, ensuring both ventilation and natural light.

3.2.5.2 Scenario Without Insulation: Baseline Envelope Configuration

Figure 3. 8 ***External Wall Composition (Without Insulation)***

The external wall of the building, modelled without any insulation layer, consists of three primary layers, as illustrated in figure 3.8:

1. Internal Plaster (Intonaco Interno):

   A 15 mm thick interior plaster layer applied to the internal face of the wall, serving as a finishing layer and offering minimal thermal resistance.

2. Masonry Block (Blocco Laterizio Semipieno):

   The core structural element is a 300 mm thick hollow clay block (dimensions: 300×245×250 mm, MS 260), providing basic thermal mass and mechanical strength. However, due to the absence of insulation, this layer allows for relatively high thermal transmittance.

3. External Plaster (Intonaco Esterno):

A 15 mm external plaster layer (cp 1000) forms the outermost finish, offering surface protection but minimal insulation performance.

The thermophysical properties and composition of each wall layer used in Scenario 1 (without insulation) are summarised in table 3.4 .

Layer No.	Material	Thickness [mm]	Density [kg/m^3]	Thermal conductivity [W/m.K]	Specific Heat [J/kg.K]
1	Internal plaster (intonaco interno)	15	1000	0,7	1000
2	Hollow brick block (Blocco laterizio sempieno)	300	260	0,6	1000
3	External plaster (Intonaco esterno)	15	1800	0,9	1000
	Total transmittance (U-value) of the wall			1,022 W/m^2·K	

Table 3. 4 ***Wall Stratigraphy Without Insulation (Scenario 1) — Layer Composition and Thermophysical Properties***

The thermal transmittance (U-value) of the floor in the configuration without insulation is 2.08 W/m²·K, indicating significant heat loss through the floor.

Figure 3. 9 ***Window Types Used in the Building Energy Simulation Model***

This figure illustrates the two main window models integrated into the energy simulation. The first type (left) is a 3-panel wooden-framed window commonly installed in most apartments of the building. It features a dark brown wood finish, double glazing, and is mounted on exterior walls, labelled “Interno” to indicate the interior view. The second type (right) is a 2-panel PVC-framed window with a white (bianco grigio) frame, transparent glass, and an aluminium handle. This model was specifically used in SUB.4, with dimensions of 0.85 m (width) and 1.15 m (height). Both window types were characterized by their thermal properties and incorporated into the Termus simulation to accurately reflect their impact on the building’s energy behaviour and heat transfer performance.

3.2.5.3 Scenario With wall Insulation: Baseline Envelope Configuration

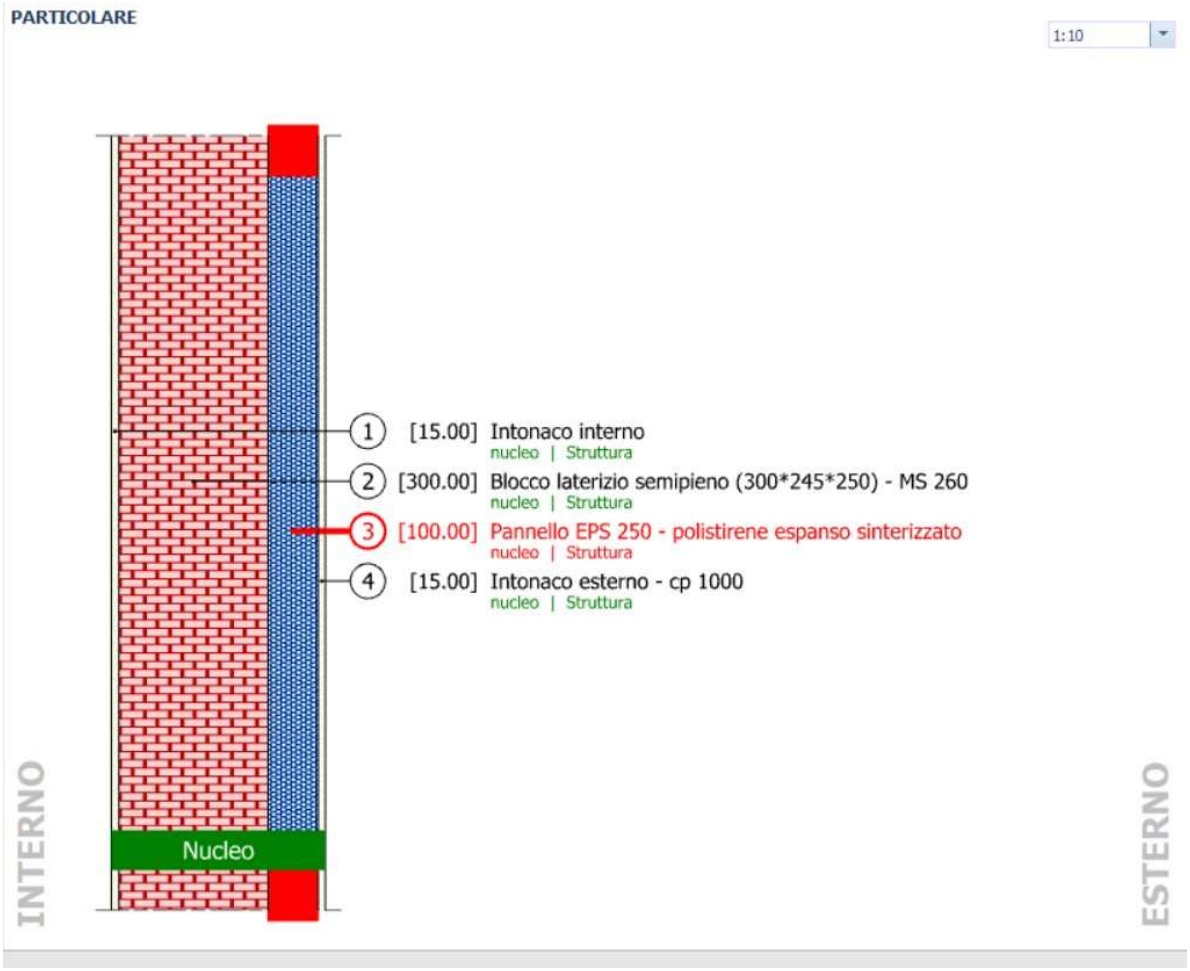

Figure 3. 10 ***External Wall Composition (With Insulation)***

1. Internal Plaster (Intonaco Interno):

   A 15 mm thick interior plaster layer is applied to the internal face of the wall, serving as a finishing layer and providing minimal thermal resistance.

2. Masonry Block (Blocco Laterizio Semipieno):

   The core structural element is a 300 mm thick hollow clay block (dimensions: 300×245×250 mm, MS 260), offering mechanical strength and basic thermal mass. Without insulation, this layer has relatively high thermal transmittance.

3. Insulation Layer (Pannello EPS 250):

   A 100 mm thick layer of expanded polystyrene (EPS 250) is placed externally. This significantly reduces thermal transmittance, improving the building's energy performance and internal comfort.

4. External Plaster (Intonaco Esterno):

A 15 mm thick external plaster layer (cp 1000) is used as the outermost finish, providing surface protection but minimal insulation benefit.

Note: All window properties, placements, and dimensions in this scenario remain the same as in the previous (non-insulated) configuration to ensure consistency in comparative analysis.

Layer No.	Material	Thickness [mm]	Density [kg/m^3]	Thermal conductivity [W/m.K]	Specific Heat [J/kg.K]
1	Internal plaster (intonaco interno)	15	1000	0,7	1000
2	Hollow brick block (Blocco laterizio sempieno)	300	260	0,6	1000
3	Insulation layer (pannello EPS 250)	100	40	0,0330	1450
4	External plaster (Intonaco esterno)	15	1800	0,9	1000
	Total transmittance (U-value) of the wall			0,2495 W/m$^{2\cdot}$K	

Table 3. 5 ***Wall Stratigraphy With Insulation (Scenario 2) — Layer Composition and Thermophysical Properties***

Table 3. 5 provides a detailed overview of the wall stratigraphy and thermophysical characteristics adopted for the insulated wall scenario.

3.2.5.4 Scenario With roof Insulation: Baseline Envelope Configuration

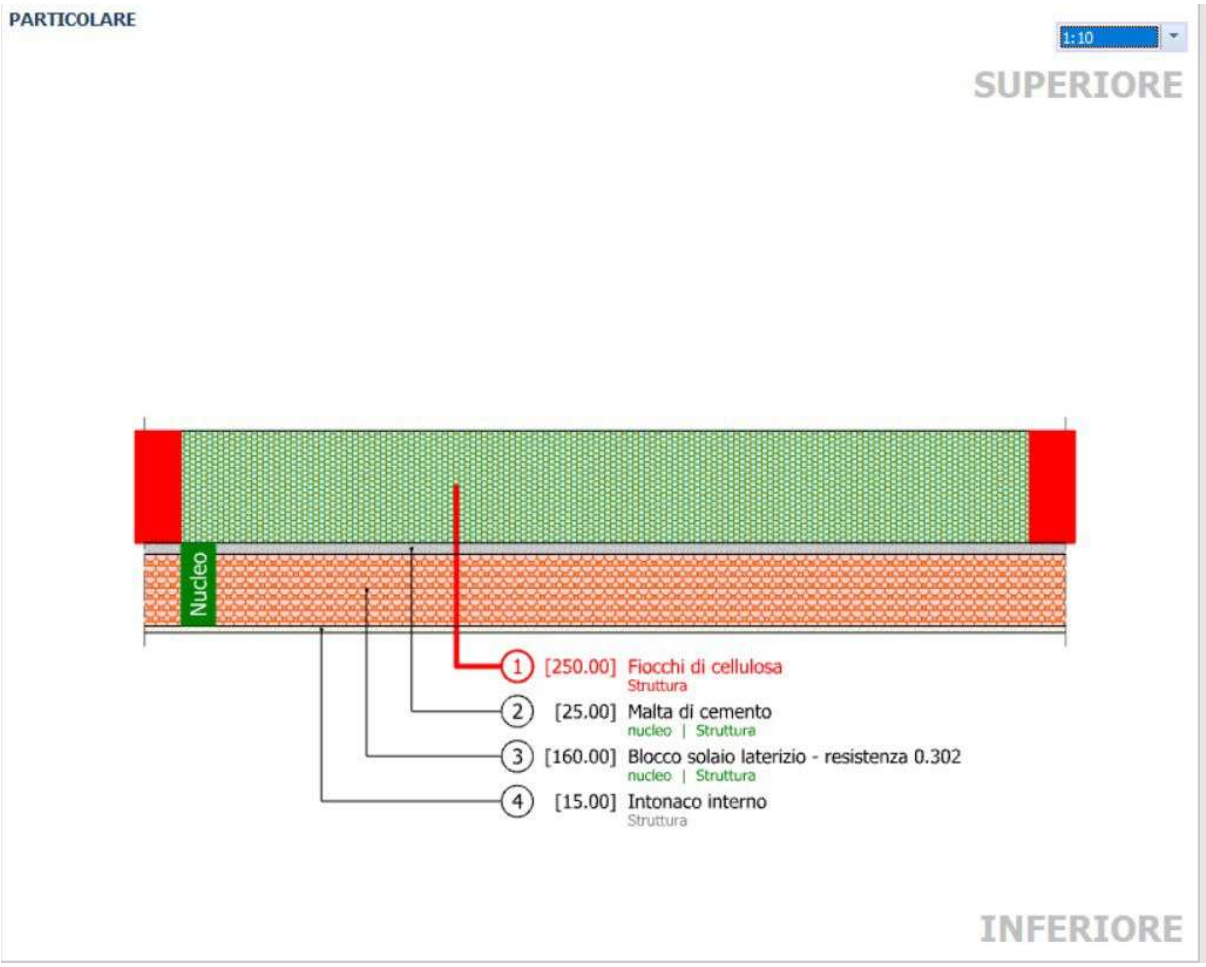

Figure 3. 11 ***Roof Structure with Cellulose Insulation Layer***

In this scenario, the building envelope is modified to include insulation in the roof only, while external walls remain uninsulated, as described previously in section 3.2.5.2. The roof structure consists of four primary layers, as illustrated in Figure 3.10:

1. Cellulose Insulation (Fiocchi di Cellulosa):

   A 250 mm thick layer of cellulose fiber insulation with thermal conductivity: 0,04 $\frac{W}{mK}$, density: 30 $\frac{kg}{m^3}$ and specific heat capacity: 2000 $\frac{J}{kgK}$ was applied to the floor of the unheated attic using a blown-in installation method. This natural insulating material provides high thermal resistance, significantly reducing heat flow through the roof.

2. Cement Mortar (Malta di Cemento):

A 25 mm layer of cement mortar lies below the insulation, functioning as a binding layer and contributing to the mechanical stability of the roof.

3. Hollow Clay Floor Block (Blocco solaio laterizio):

   The main structural element is a 160 mm thick hollow clay block, offering thermal mass and a thermal resistance of 0.302.

4. Internal Plaster (Intonaco Interno):

   A 15 mm interior plaster layer finishes the underside of the roof, offering minimal insulation but completing the internal appearance.

Layer No.	Material	Thickness [mm]	Density [kg/m^3]	Thermal conductivity [W/m.K]	Specific Heat [J/kg.K]
1	Cellulose Insulation (Fiocchi di Cellulosa)	250	30	0,04	2000
2	Cement Mortar (Malta di Cemento)	25	2000	0,7	1000
3	Hollow Clay Floor Block (Blocco solaio laterizio)	160	-	-	1000
4	Internal Plaster (Intonaco Interno):	15	1400	0,7	1000
	Total transmittance (U-value) of the floor			0,1479 W/m^2·K	

Table 3. 6 ***Roof Stratigraphy with Insulation (Scenario 4) — Layer Composition and Thermophysical Properties***

3.2.5.5 Scenario With wall and roof Insulation: Baseline Envelope Configuration

This scenario includes both wall and roof insulation. Wall and roof layers are the same as previously defined in individual insulation scenarios.

All windows remain unchanged compared to the previous models.

3.2.5.6 Initial Setup in Geotermus

3.2.5.6.1 Climatic Conditions and Boundary Inputs

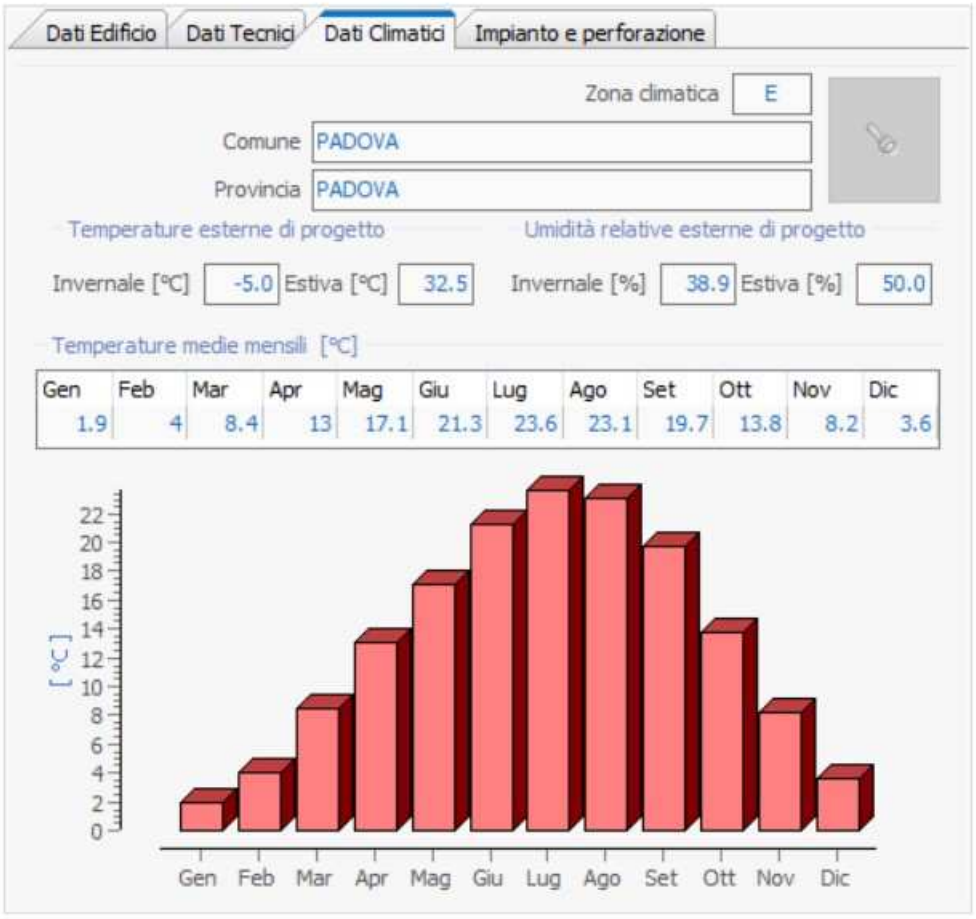

Figure 3. 12 ***Climatic Conditions Setup in Geotermus for Padova (Zone E)***

This image shows the climatic data automatically loaded in Geotermus after selecting Padova as the project location. The software defines the climatic zone (E) and assigns both design temperatures (−5.0 °C in winter and 32.5 °C in summer) and average monthly temperatures for the entire year. These values are essential for accurately estimating the seasonal heating and cooling demands of the building and directly influence the geothermal sizing process. The provided climate data ensures that the system is correctly tailored to real environmental conditions in Padova.

Figure 3. 13 ***Monthly Heating and Cooling Energy Demand Profile for SUB 3 (Without Insulation)***

This figure illustrates the monthly energy demand profile for SUB 3 without any thermal insulation, as entered Geotermus just as an example. The data previously calculated in Termus has been imported to define the required heating (riscaldamento) and cooling (raffrescamento) loads for each month. The red bars represent heating energy needs, peaking in January and December, while the blue bars show cooling demands, mostly observed during the summer months like July. The chart also displays the design powers: 5.9 kW for heating and −5.1 kW for cooling, which are critical inputs for sizing the geothermal heat exchanger.

It is important to note that the energy required for domestic hot water (DHW) has been excluded from this analysis, as it may be produced through alternative systems.

In the following the proper heat pump settings was selected for the geothermal system, chosen from a manufacturer's catalogue [24] as suitable for residential applications like the studied apartment in Padova.

Parameter	Value
Heating capacity at 10/55 degC	7,5 [kW]
Refrigerant type / volume	R407C / 1.16 [kg]
Sound pressure at 1 m	21-28 dB
Power supply	230 V / 50 Hz

COP at 10/55 degC (heating mode)	3,5
EER (cooling mode)	4
Energy efficiency label	A+++

Table 3. 7 ***Main Technical Specifications of the Selected Heat Pump (NIBE S1155 Inverter – 1–6 kW)***

Figure 3. 14 ***Coaxial Heat Exchanger Configuration: Pipe Dimensions Defined in Geotermus***

In this figure, the coaxial heat exchanger configuration is defined within the Geotermus software. The selected dimensions outer and inner diameters and wall thickness are the result of previous optimization work carried out using COMSOL simulations. This configuration includes:

- Internal pipe outer diameter (di): 63.0 mm
- Internal pipe thickness (ti): 5.4 mm
- External pipe outer diameter (do): 88.9 mm
- External pipe thickness (to): 3.6 mm

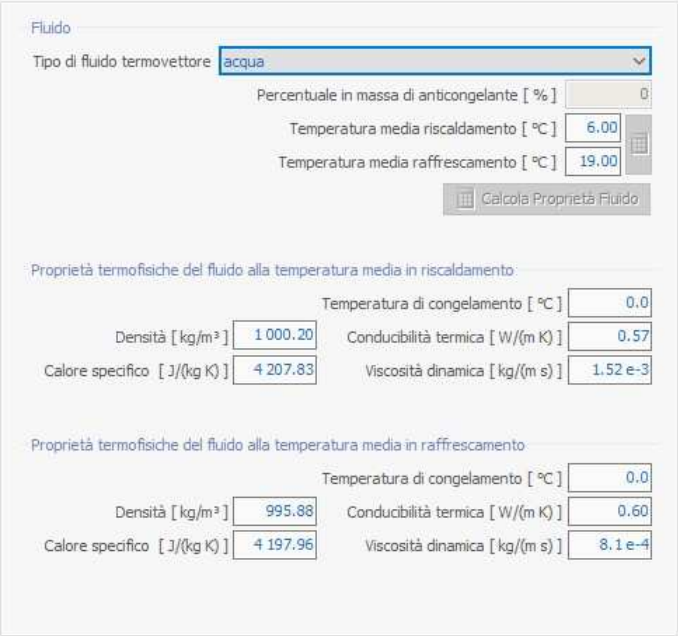

Figure 3. 15 ***Selection of Water as the Working Fluid and Its Thermophysical Properties in GeoThermus***

Figure 3.15 presents the thermophysical properties of the heat transfer fluid used in the simulations, which is water (*acqua*). The data is extracted from the Termus interface and corresponds to two operating conditions: heating and cooling. No antifreeze was added, as indicated by the 0% glycol concentration. For the heating mode, an average fluid temperature of 6 °C was set, while for cooling it was 19 °C. At these conditions, the software calculates the following fluid properties: density, specific heat, thermal conductivity, and dynamic viscosity. These values are essential for accurately modeling the thermal exchange between the circulating fluid and the ground in both seasonal modes.

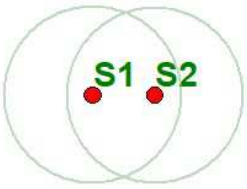

Figure 3. 16 ***Parallel Configuration of Two Coaxial Geothermal Probes (S1 and S2)***

This configuration represents a sample case for SUB 10 under the no-insulation scenario, where Geotermus simulation results were used to define the geothermal system layout. Based on the annual heating and cooling energy demands previously calculated in Termus, the software determined that

two coaxial geothermal heat exchangers (S1 and S2) are required to meet the building's thermal needs. These exchangers are arranged in a parallel configuration with 7m distance from each other, as depicted in the figure, ensuring balanced thermal load distribution and effective system operation. The required drilling depths for each scenario will be presented in the Results chapter. These values indicate how the presence or absence of insulation (in walls, roof, or both) impacts the total borehole length needed to meet the building's heating and cooling demands.

4

Results and Discussion

4.1 Model Validation

To ensure the accuracy of the numerical model developed in COMSOL Multiphysics, a validation was conducted by comparing simulation results with real operational data obtained from a coaxial borehole heat exchanger installed in Putte, Belgium[25]. The monitored system served a two-level residential building of 160 m² with a wooden structure and straw bale walls. Located approximately 20 m from a separate veterinary studio. The geothermal system includes six borehole heat exchangers (four co-axial and two double U-tube) with a total length of 480 meters. Additional components include solar collectors, a thermal buffer tank, a PV system on the veterinary studio roof, and full thermal and electrical metering. This system was monitored during the winter season of 2019, and the data was provided by RED srl, the company where this thesis project was carried out as part of an internship.

The geometry of the real system included an outer pipe made of stainless steel, with an outer diameter of 76.1 mm and a wall thickness of 3.6 mm, and an inner pipe made of HDPE (High-Density Polyethylene) with an outer diameter of 32 mm and a thickness of 2 mm. The total length of the borehole was 80 meters. This geometry and material configuration were replicated in COMSOL for the validation phase.

Regarding the boundary conditions, the average annual surface temperature was set to 11°C, while the subsurface temperature at 85 meters depth was set to 13.4°C, following local geothermal gradient data. [24] The fluid used in the system was pure water, and the average volumetric flow rate observed during the winter season was used as a constant input in the simulation. The inlet temperature of the fluid was not fixed but applied as a variable time-dependent boundary condition, using the real hourly temperature data collected from the system.

The main validation metric was the return (outlet) temperature of the fluid, which was measured over time in the real system and computed in COMSOL simulations. A comparison was made by plotting both time series on the same graph, and the results showed that the simulated data closely followed the field measurements, with only minor deviations.

To quantify the level of agreement, two statistical indicators were calculated:

- Mean Bias Error (MBE)

- Coefficient of Variation of the Root Mean Square Error (CVRMSE)

Both indicators were within the acceptable limits set by ASHRAE Guideline 14 for **hourly** simulations, which are:

- |MBE| ≤ 10%
- CV(RMSE) ≤ 30%

The good alignment between simulated and measured data confirms the reliability and accuracy of the numerical model developed in COMSOL, thus validating its application for evaluating different coaxial configurations and their performance.

$$\mathrm{MBE}(\%) = \frac{100}{n} * \sum_{i=1}^{n} \frac{M_i - S_i}{\bar{M}} \qquad (4\text{-}1)$$

M_i: Measured value (e.g., real outlet temperature)

S_i: Simulated value

$\bar{M}$: Mean of measured values

n: $Number\ of\ data\ ponts$

$$\mathrm{CV(RMSE)}(\%) = \frac{100}{\bar{M}} * \sqrt{\frac{1}{n}\sum_{i=1}^{n}(M_i - S_i)^2} \qquad (4\text{-}2)$$

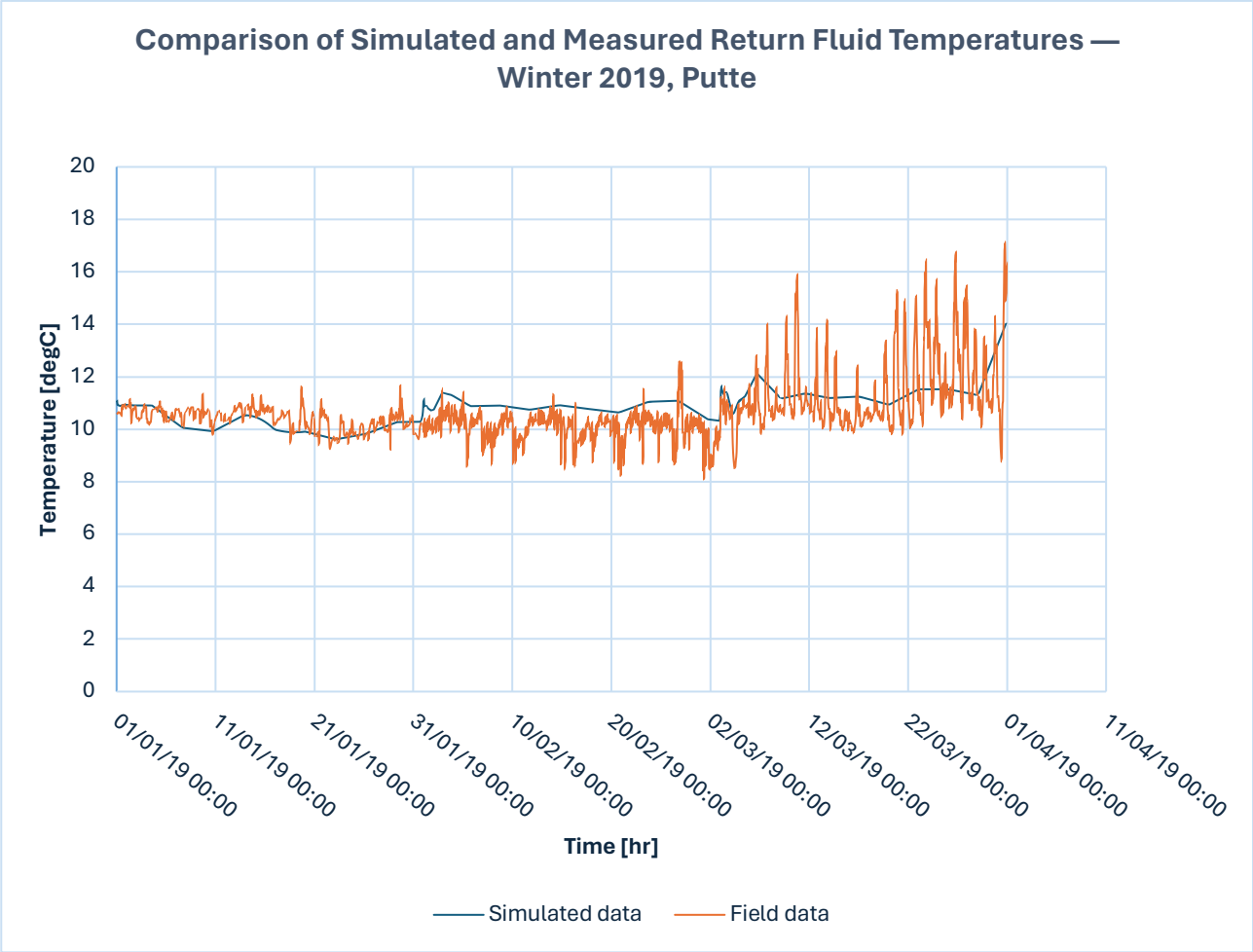

Figure 4. 1 ***Comparison Between Simulated and Measured Return Fluid Temperatures in Winter 2019 (Mechelen)***

The validation was conducted by comparing the simulated return fluid temperatures from the COMSOL® model with real field data collected in Putte during Winter 2019. As shown in Figure 4.1, the simulated temperatures follow the trend of the measured data with minor deviations. To assess the model's accuracy, Mean Bias Error (MBE) and Coefficient of Variation of the Root Mean Square Error (CV(RMSE)) were calculated as recommended by ASHRAE Guideline 14,

- CV(RMSE): 9.79%
- MBE: -1.81%$

According to ASHRAE:

- For hourly data, MBE should be within ±10% and CV should be below 30%.

These values fall well within the acceptable range, indicating that the simulation is in good agreement with real data and the model can be considered validated for this specific case.

Some fluctuations in the measured return temperature, especially toward the end of the simulation, are likely due to the on/off cycling of the heat pump and natural ground temperature variations. Despite these, the simulation accurately follows the overall trend, confirming the model's reliability under real operating conditions

4.2 Thermal and Velocity Field Visualization

4.2.1 Temperature distribution for heating purposes

Figure 4.2 shows the temperature distribution across the entire coaxial system, including the inner pipe, outer pipe, cement layer, and surrounding ground. The cold fluid enters the system through the annular space around the inner pipe and gradually gains heat as it moves downward. As it returns upward through the inner pipe, the fluid temperature increases due to heat transfer from the surrounding soil. The image clearly shows that the return fluid in the inner pipe reaches a higher temperature than the injected fluid, demonstrating effective thermal exchange within the system.

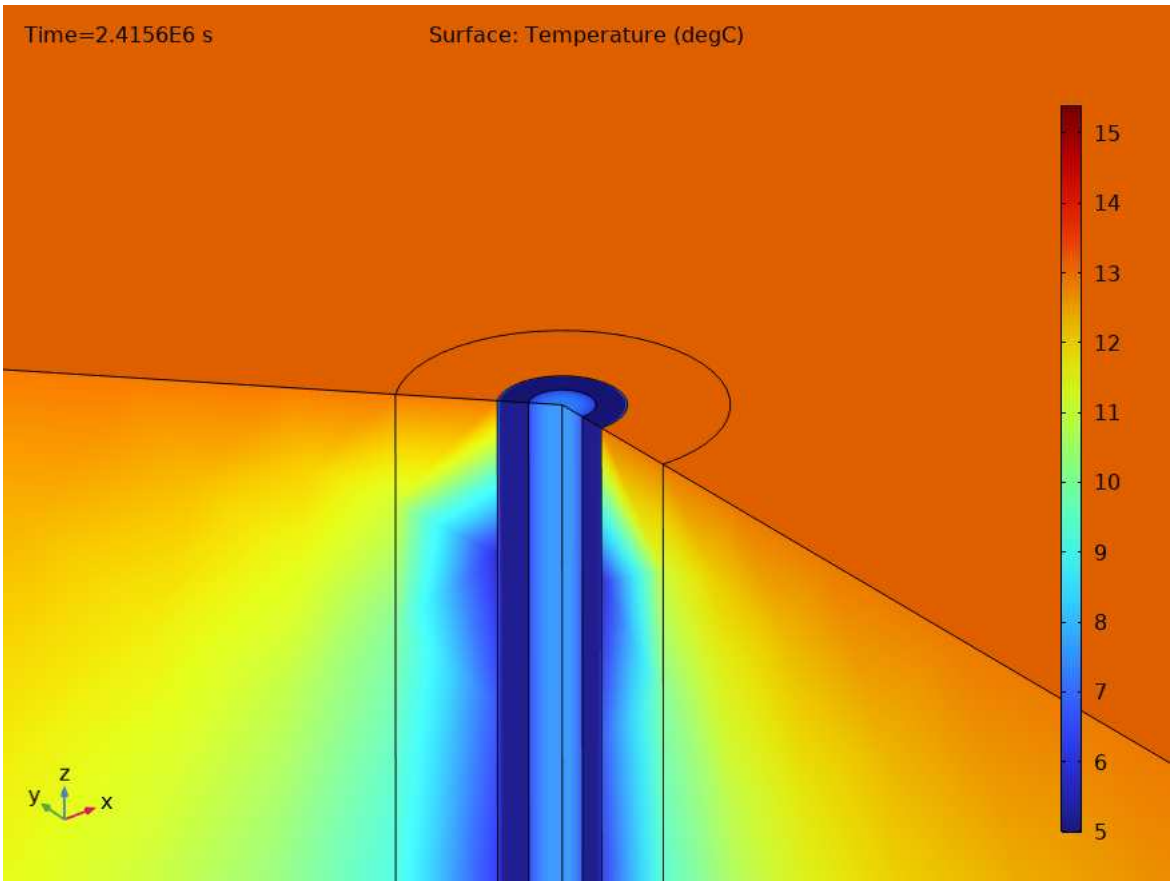

Figure 4. 2 ***Temperature Profile in the Upper Section of the Coaxial Borehole Heat Exchanger during Heating Mode***

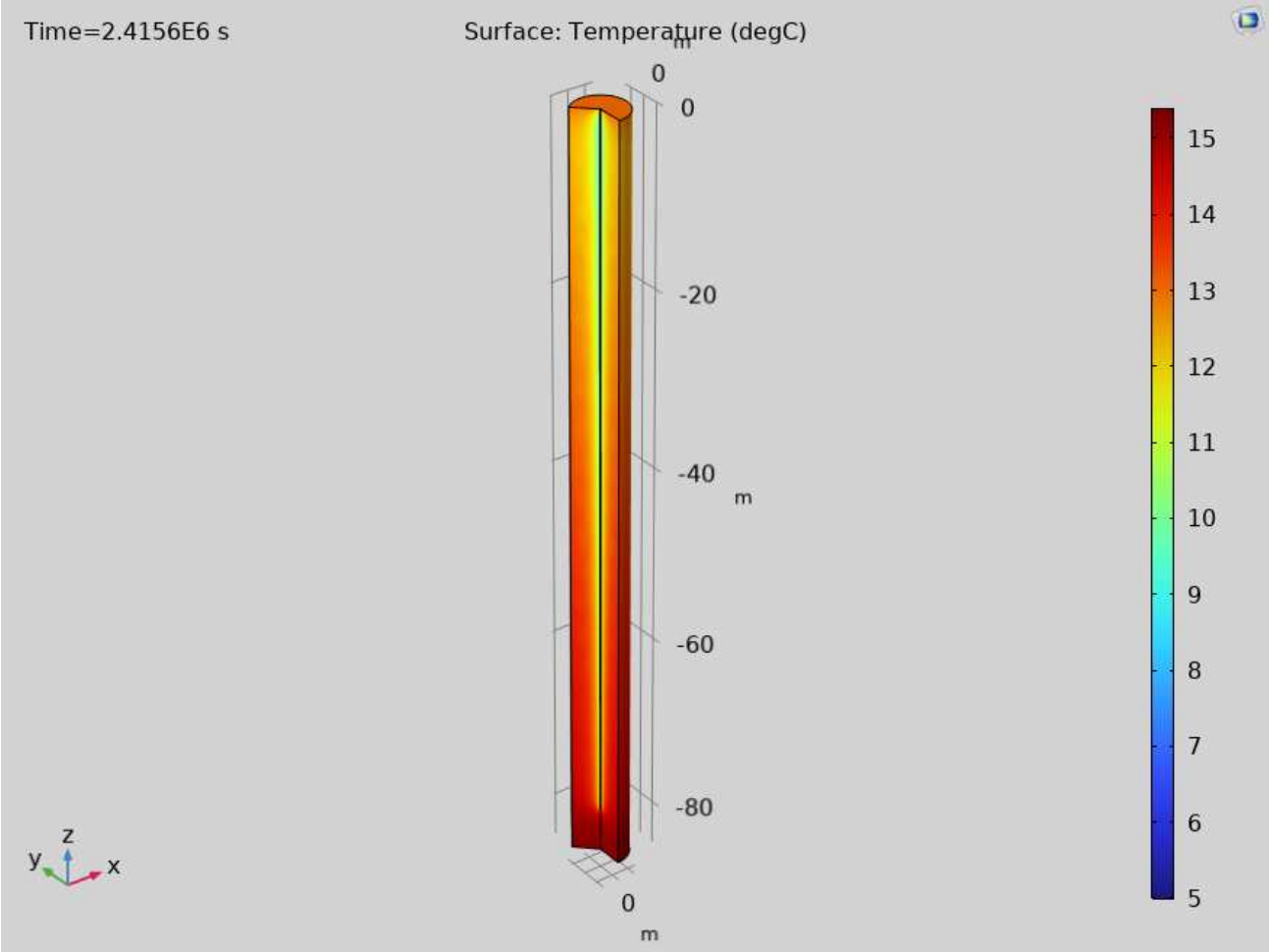

Figure 4. 3 ***Temperature Distribution Along the Entire Borehole Geometry***

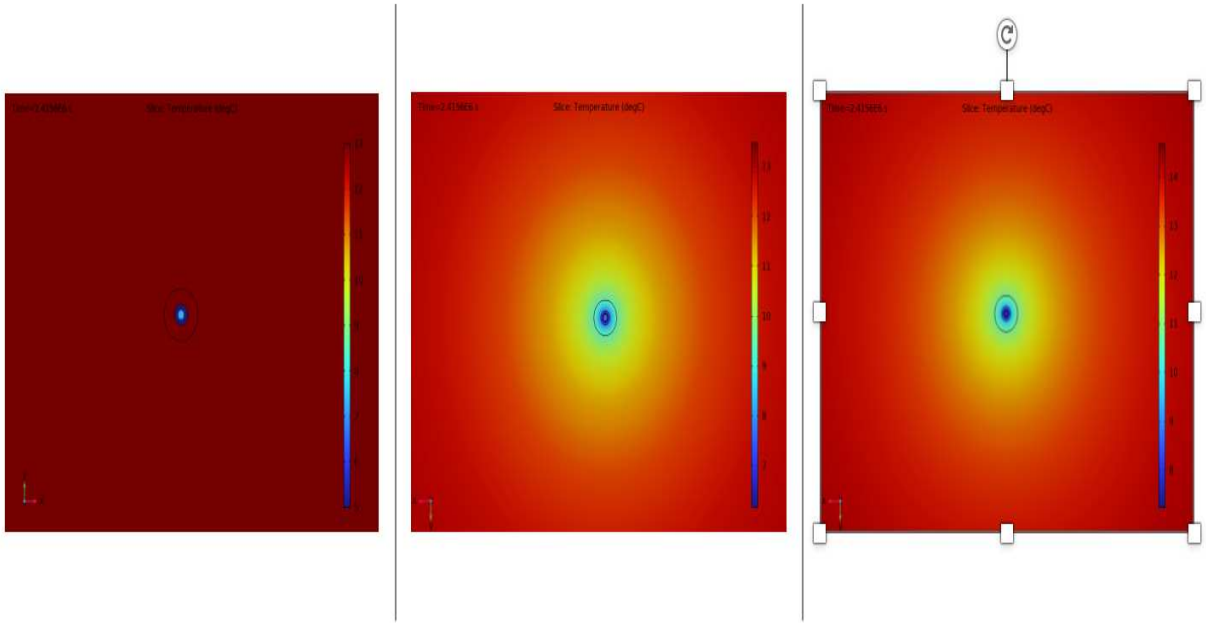

Figure 4. 4 ***Temperature Distribution Around the Borehole at Three Depths (0 m, 40 m, and 80 m) After One-Month Heating Operation***

To gain a better understanding of the heat transfer behaviour within the coaxial borehole heat exchanger (CBHE) during the one-month heating period, temperature contour plots were extracted at three representative depths from left to right: the top (0 m), mid-depth (40 m), and the bottom of the well. These visualizations allow qualitative assessment of the thermal plume development over time and depth.

Each image includes the inner pipe, outer pipe, cement layer, and the surrounding ground. The central circular region represents the inner flow pipe, while the annular area shows the outer pipe, with the cemented zone and soil beyond it. Temperature gradients can be observed extending outward from the heat exchanger.

At the top (0 m), the heat transfer is limited, and the temperature rise around the pipe is small. At 40 m, the heat spreads more widely, showing stronger interaction with the soil. At the bottom (80 m), the temperature field is the largest, meaning more heat has been transferred into the ground. This confirms that deeper sections of the borehole contribute more to heat exchange.

4.2.2 Velocity Magnitude Distribution in the Inner Pipe and Annular Region of the CBHE

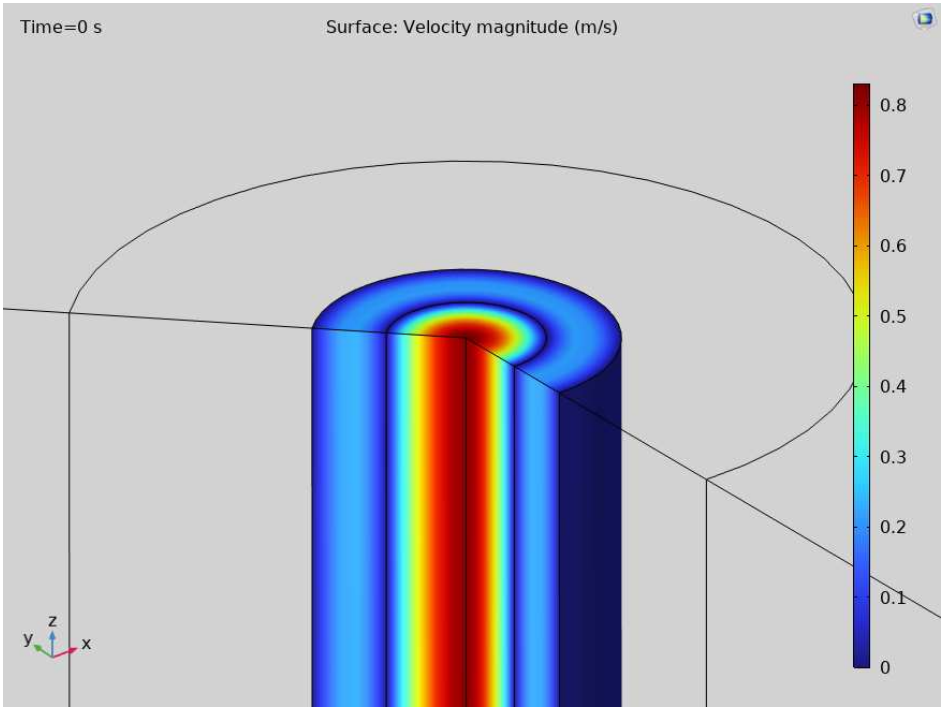

Figure 4. 5 ***Velocity magnitude distribution in the inner pipe and annular space of the coaxial borehole heat exchanger***

This figure shows the velocity magnitude distribution of the working fluid across both the inner pipe and the surrounding annular space at the upper part of the coaxial borehole heat exchanger (CBHE). The highest velocity occurs at the centre of the inner pipe and decreases toward the wall due to the no-slip boundary condition, forming a typical parabolic profile. In the annular region, a similar gradient is visible, with velocity dropping near both the inner and outer pipe walls. This distribution reflects fully developed internal pipe flow and confirms that the velocity varies significantly with radial position in both flow paths.

4.3 Simulation Results

The simulation results presented in this section are based on the parametric configurations described in table 3.3. Eleven coaxial heat exchanger models with varying inner and outer pipe diameters were tested under identical heating conditions to evaluate the effect of geometry on thermal performance. The following results highlight the key trends and comparative performance among these configurations.

4.3.1 Thermal Performance Under Heating Mode

In the first part all simulations were conducted under heating mode conditions, using a constant inlet fluid temperature of 5°C and a fixed volumetric flow rate of 12 L/min. The thermal boundary conditions reflected the typical temperature gradient in Padova, Italy, where the surface ground temperature was set to 13°C, and the temperature at 85 meters depth was 15.4°C.

The objective of this simulation campaign was to analyse the impact of geometric parameters particularly the pipe diameters on the thermal output performance of the CBHE. The outlet temperature and transferred thermal power were monitored over a one-month period to compare the effectiveness of each design.

The graph in Figure 4.6 illustrates the outlet fluid temperature over one month for 11 different coaxial borehole configurations, all simulated under the same operating conditions: an inlet temperature of 5°C and a constant flow rate of 12 L/min. As shown, all models exhibit a rapid temperature drop at the beginning, followed by a gradual stabilization.

Among the models, Model 1 (Øout-88.9mm_Øin-63mm, with the largest inner diameter) consistently maintains the highest outlet temperature, while Model 11 (Øout-48.3 mm_Øin-25mm, with the smallest inner diameter) shows the lowest. This trend highlights that larger inner pipe diameters improve return temperature performance in heating applications, likely due to increased internal flow area and lower heat loss to the annular space.

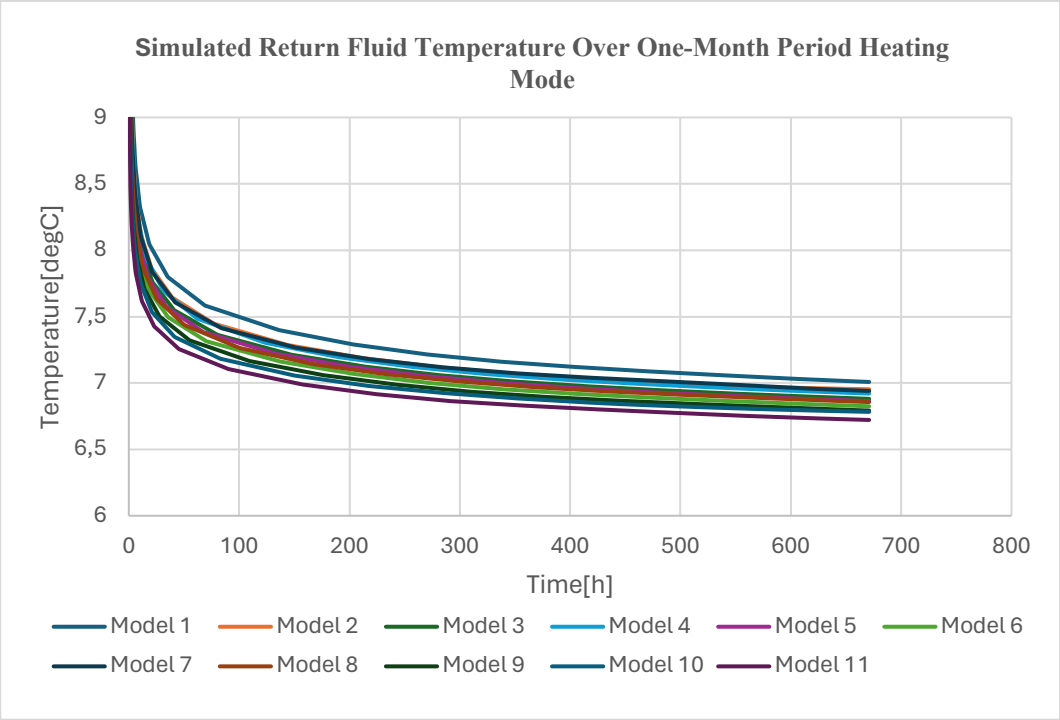

Figure 4. 6 ***Simulated Outlet Fluid Temperature Over One-Month Period for 11 Coaxial Borehole Heat- Exchanger (CBHE) Configurations in Heating Mode***

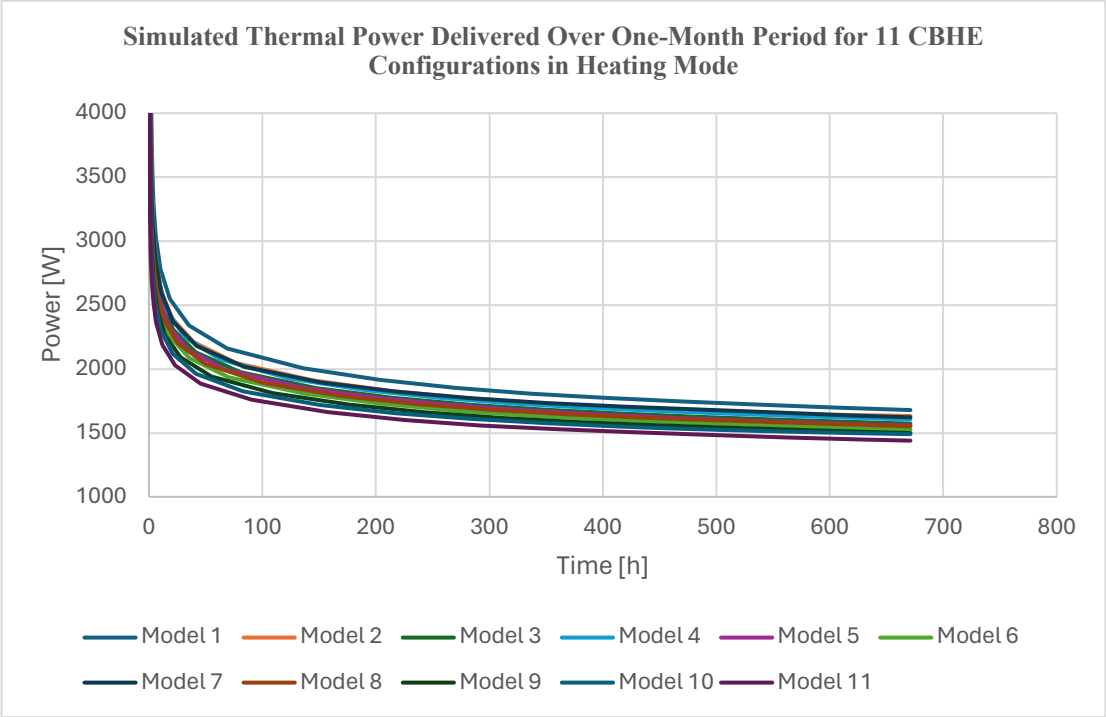

Figure 4. 7 ***Simulated Thermal Power Delivered Over One-Month Period for 11 CBHE Configurations in Heating Mode***

The thermal power generated from the geothermal system can be calculated using the standard equation:

$$\dot{Q} = \dot{m} \cdot c_p . \Delta T$$

- $\dot{Q}$ is the thermal power [W],
- $\dot{m}$ is the mass flow rate [kg/s],
- c_p is the specific heat capacity of the fluid [J/kg·K],
- ΔT is the temperature difference between the outlet and inlet fluid [K].

Since the mass flow rate and specific heat capacity are constant in all configurations, the temperature difference (ΔT) becomes the key factor. As shown in Figure 4.7, Model 1(Øout-88.9mm_Øin-63mm) provides the highest power output because it maintains the largest temperature difference over time. This is primarily due to its larger inner pipe diameter, which reduces internal heat loss between downward and upward flows, thereby preserving the return fluid's thermal energy and improving overall performance.

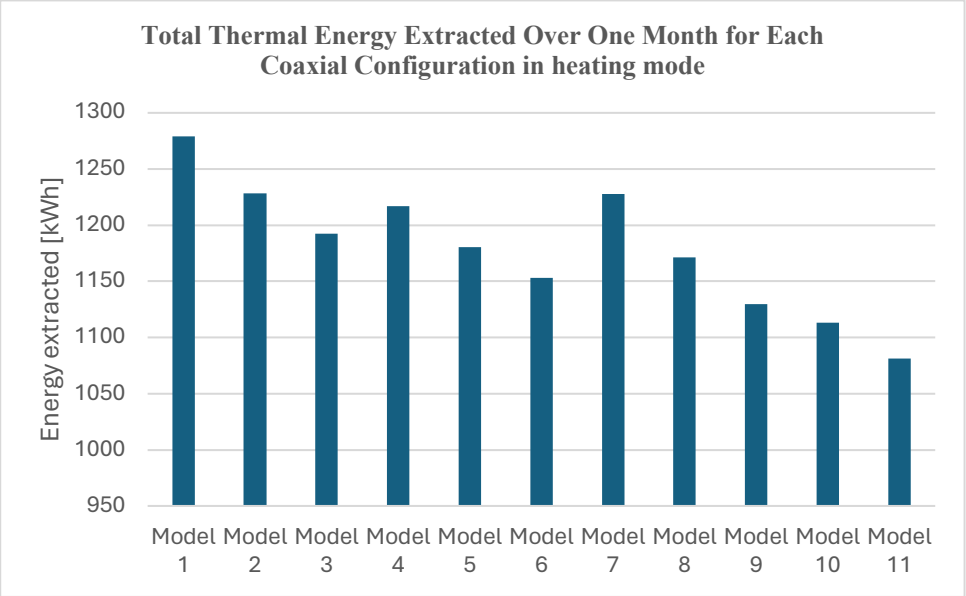

Figure 4. 8 ***all Thermal Energy Extracted Over One Month for Each Coaxial Configuration in heating mode***

Figure 4.8 shows the total thermal energy extracted over one month for each coaxial borehole configuration in heating mode. Model 1 gives the highest energy output, while Model 11 gives the lowest. The results show that the dimensions of the pipes have a big effect on how much energy can be extracted from the ground.

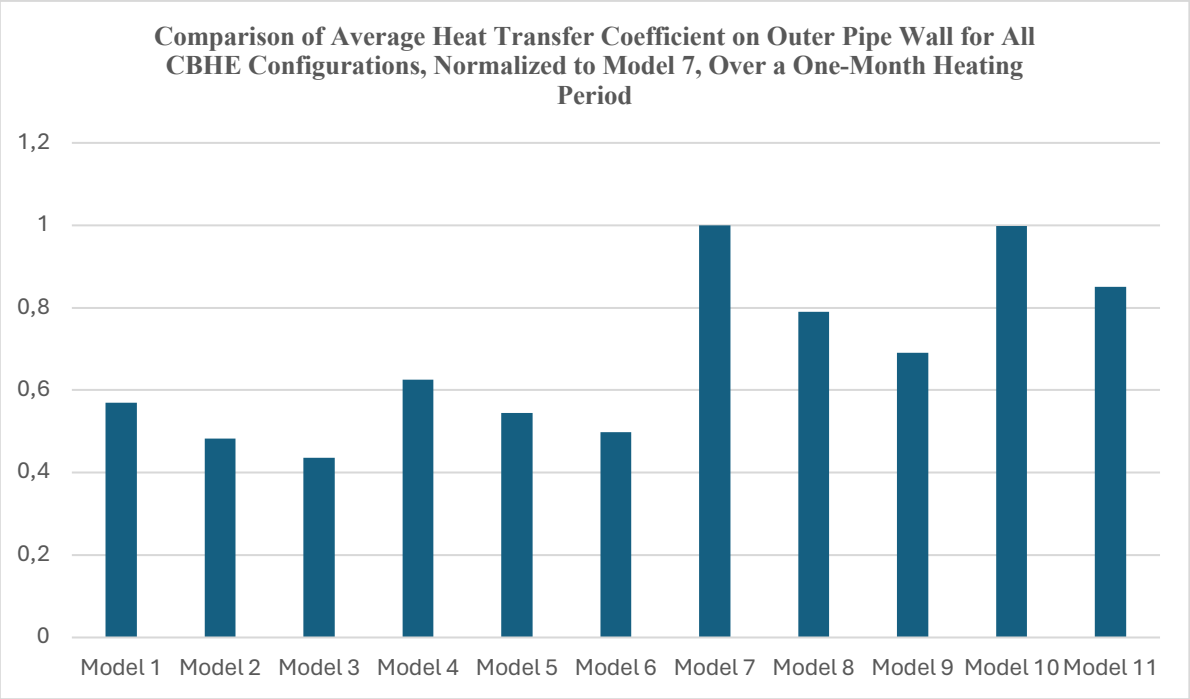

Figure 4. 9 ***Comparison of average heat tranfer coefficient on outer pipe wall for all CBHE configurations, normalized to Model 10, over a one-month heating period***

Figure 4.9 shows the heat transfer coefficient at the outer pipe wall over time for all configurations. Models with a narrower annular space, like Model 7(Øout-60.3 mm_Øin-50mm), exhibit higher heat transfer coefficients due to increased fluid velocity and turbulence in the annular region. However, the shorter residence time in the ground reduces the total exchanged energy.

Conversely, Model 1 (Øout = 88.9 mm, Øin = 63 mm), which has a larger inner pipe diameter, allows greater flow area for the returning fluid. While a larger diameter reduces internal convective heat transfer due to lower velocity, it also minimizes unwanted heat exchange between the outgoing and returning streams within the borehole. As a result, Model 1 demonstrates better overall thermal performance by limiting internal recirculation and enhancing effective heat transfer to the ground.

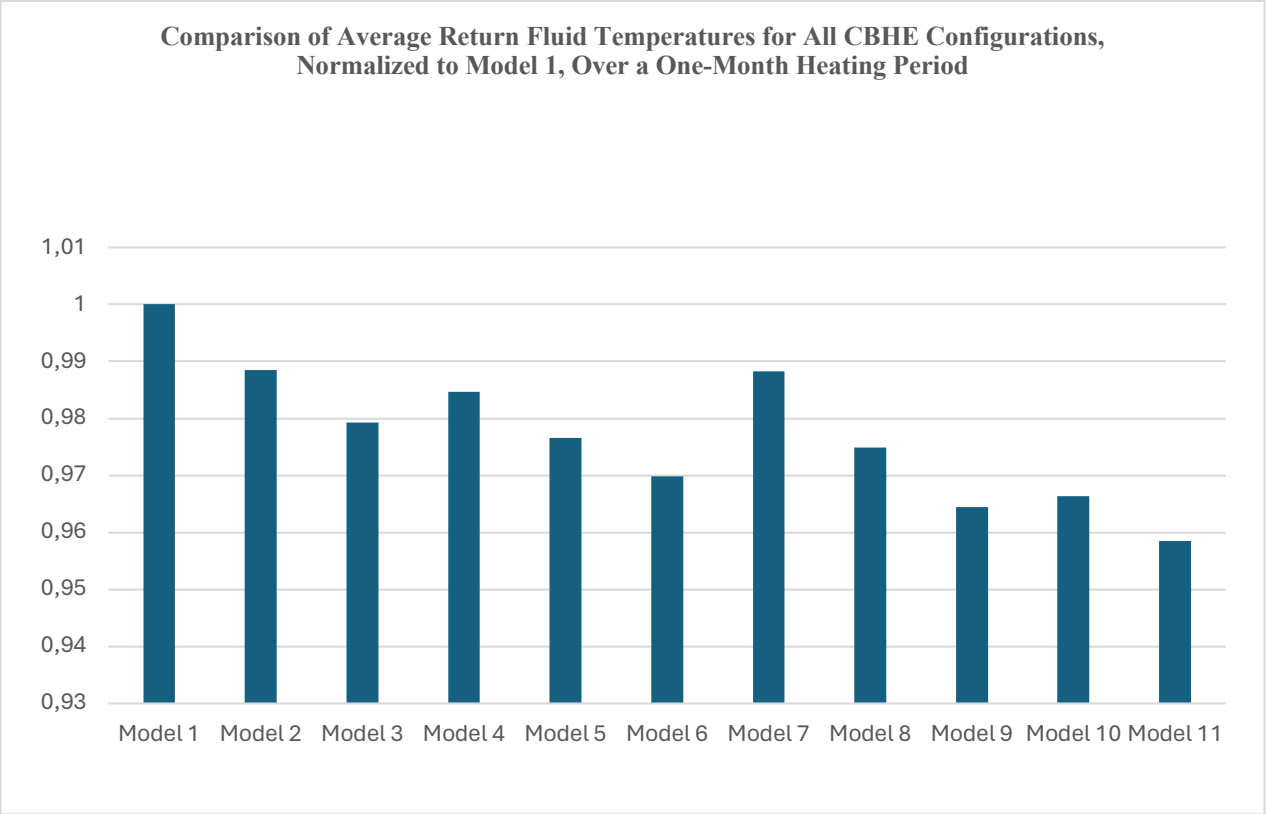

Figure 4. 10 ***Comparison of Average Return Fluid Temperatures for All CBHE Configurations, Normalized to Model 1, Over a One-Month Heating Period***

Figure 4.10 presents the normalized average return fluid temperatures for all CBHE configurations over a one-month heating period. The results are referenced to Model 1, which showed the highest performance, allowing a direct comparison of the relative efficiency of each geometry in maintaining outlet temperature.

4.3.2 Thermal Performance Under Cooling Mode

In the next stage of the analysis, simulations were performed for cooling purposes by setting the inlet temperature to 20 °C and maintaining a constant flow rate of 12 L/min. As shown in Figure 4.11, all configurations exhibit an increase in outlet fluid temperature over time, reflecting heat gain from the surrounding ground. Among all models, Model 1(Øout = 88.9 mm, Øin = 63 mm) consistently achieved the lowest outlet temperatures, indicating the highest cooling efficiency. This behaviour can be attributed to its larger inner pipe diameter, which reduces internal heat loss between the injected and return fluids, enhancing the system's thermal separation and cooling performance.

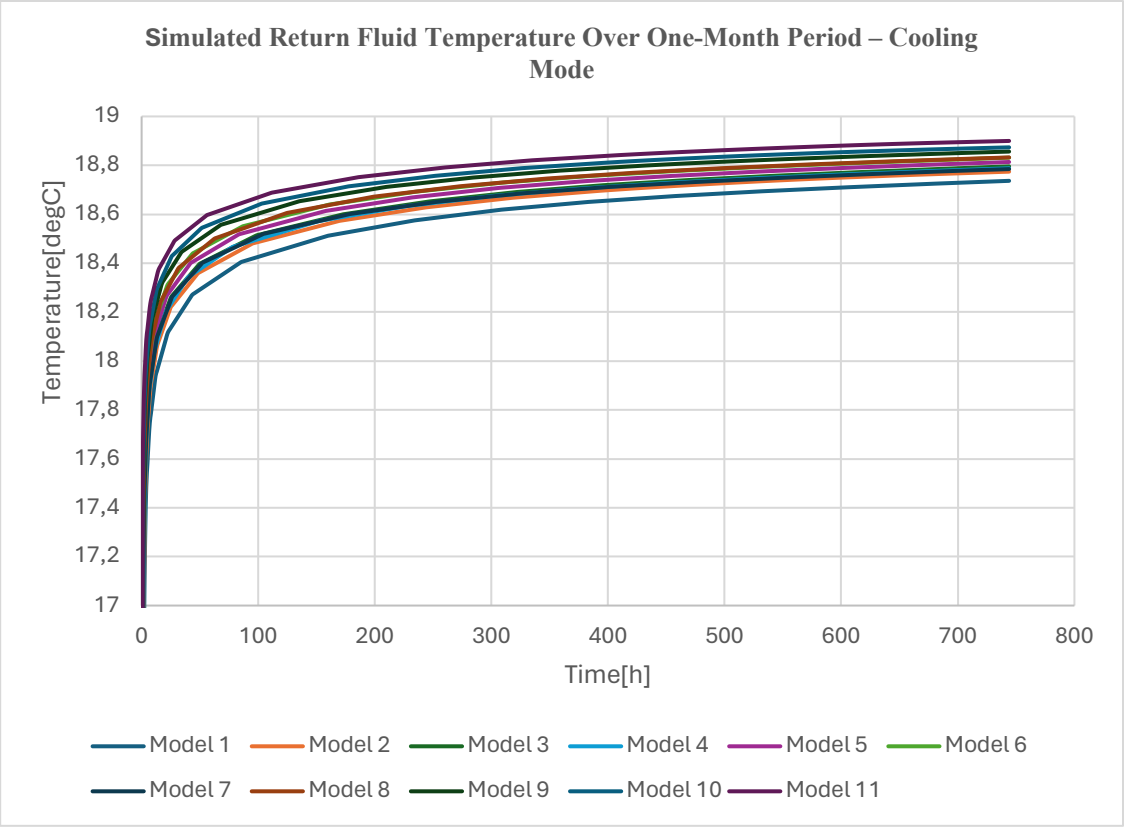

Figure 4. 11 ***Simulated Outlet Fluid Temperature Over One-Month Period for 11 Coaxial Borehole Heat- Exchanger (CBHE) Configurations in Heating Mode***

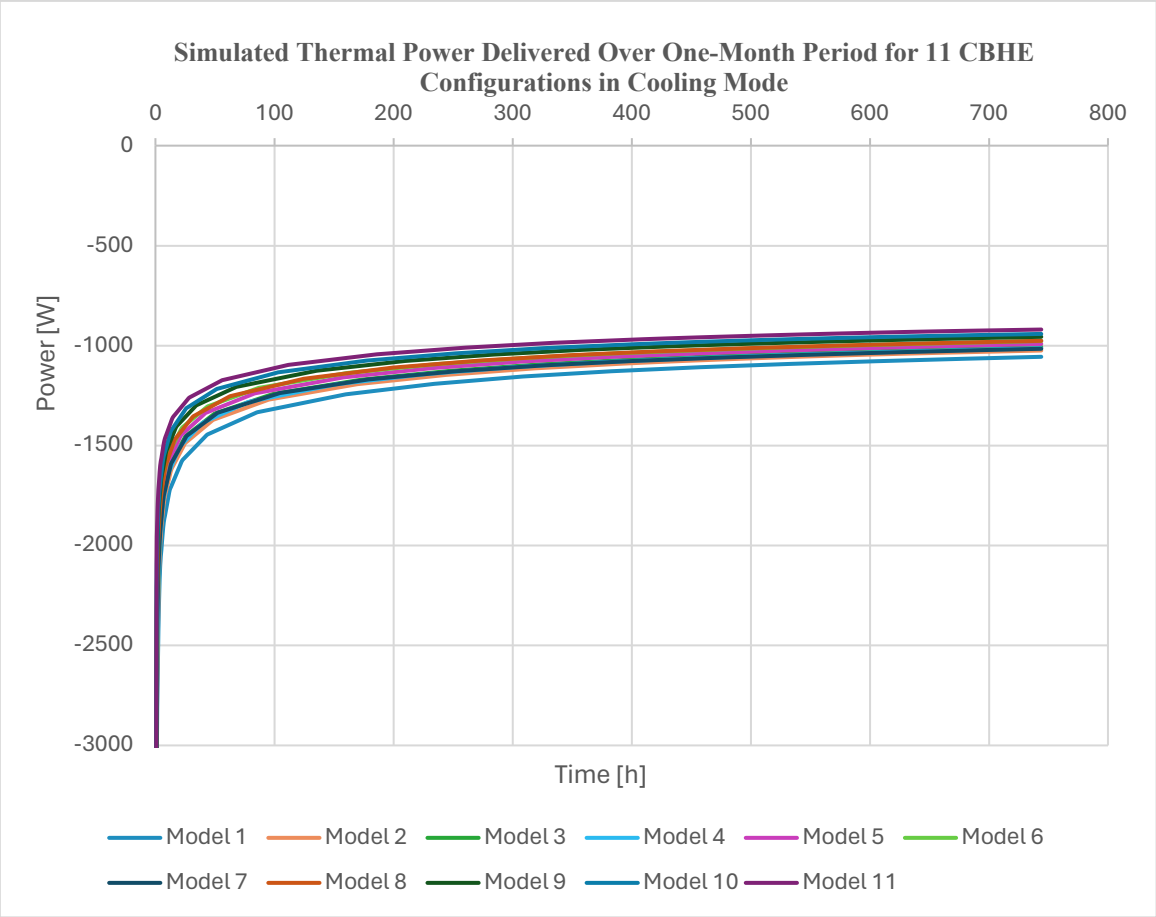

Figure 4. 12 ***Simulated Thermal Power Delivered Over One-Month Period for 11 CBHE Configurations in Cooling Mode***

In figure 4.12, the power values are shown for all configurations under cooling conditions (inlet temperature of 20 °C and flow rate of 12 L/min). In cooling mode, the injected fluid is warmer than the surrounding soil, so heat flows from the fluid to the ground, and the system acts as a heat sink. This heat extraction is conventionally reported as negative thermal power. Over time, the extracted power gradually decreases as the fluid temperature approaches thermal equilibrium with the soil. Among all cases, Model 1 achieves the most negative power, which means it rejects the most heat from the ground. This is mainly due to its larger inner pipe, which helps maintain a stronger temperature difference and reduces heat loss to the injected flow. In the cooling mode, the negative sign in the power graph indicates that heat is being released from the fluid to the ground.

4.3.3 Impact of Inlet Fluid Flow Rate on Thermal Performance in Heating Mode for the Optimal Configuration (Model 1)

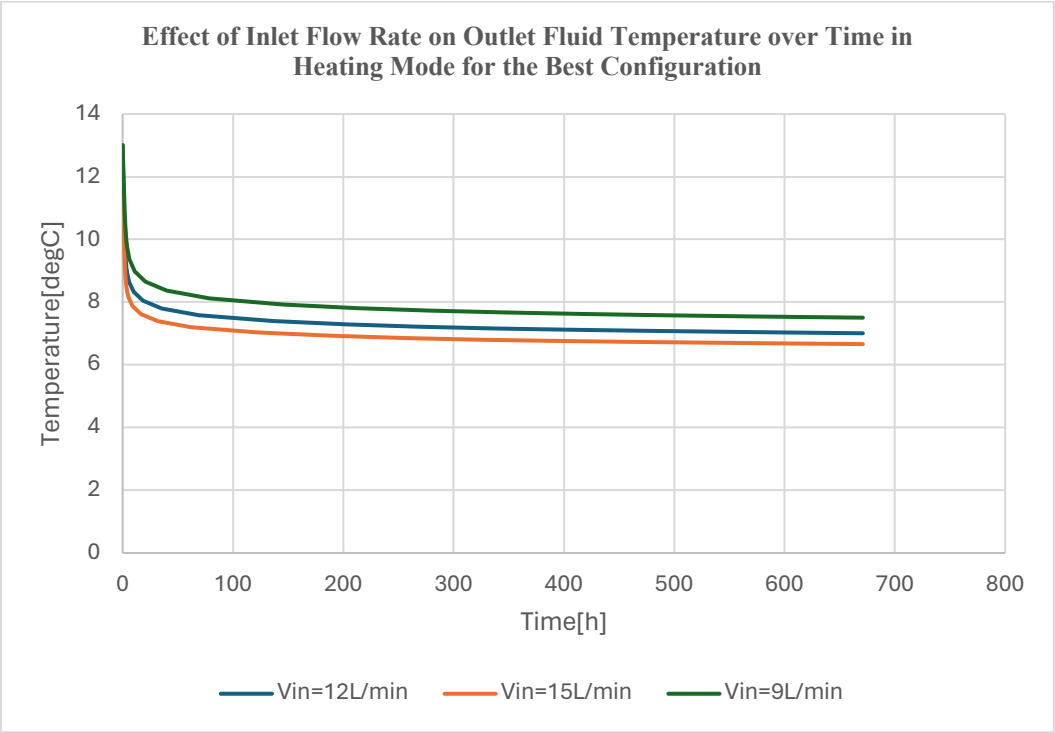

Figure 4. 13 ***- Effect of Inlet Fluid Flow Rate on Outlet Fluid Temperature over Time in Heating Mode for the Best Configuration***

To evaluate the effect of inlet flow rate on system thermal behaviour, simulations were carried out on the best-performing configuration which was Model 1 (Øout = 88.9 mm, Øin = 63 mm) using three different volumetric flow rates: 9, 12, and 15 L/min, while keeping the inlet temperature fixed at 5 °C. As shown in Figure 4.13 , the outlet temperature slightly decreases as the flow rate increases. This is because lower flow rates allow the fluid to spend more time inside the borehole, enabling greater heat absorption from the surrounding ground. In contrast, higher flow rates reduce the residence time, limiting the heat transfer to the fluid. These results confirm that, for heating purposes, higher inlet flow rates lead to greater thermal power output, as shown in Figure 4.14. Although lower flow rates may slightly increase the outlet fluid temperature due to longer residence time, the total thermal power generated by the system is maximized at higher flow rates (e.g., 15 lit/min), due to the larger heat transfer rate associated with increased fluid mass flow.

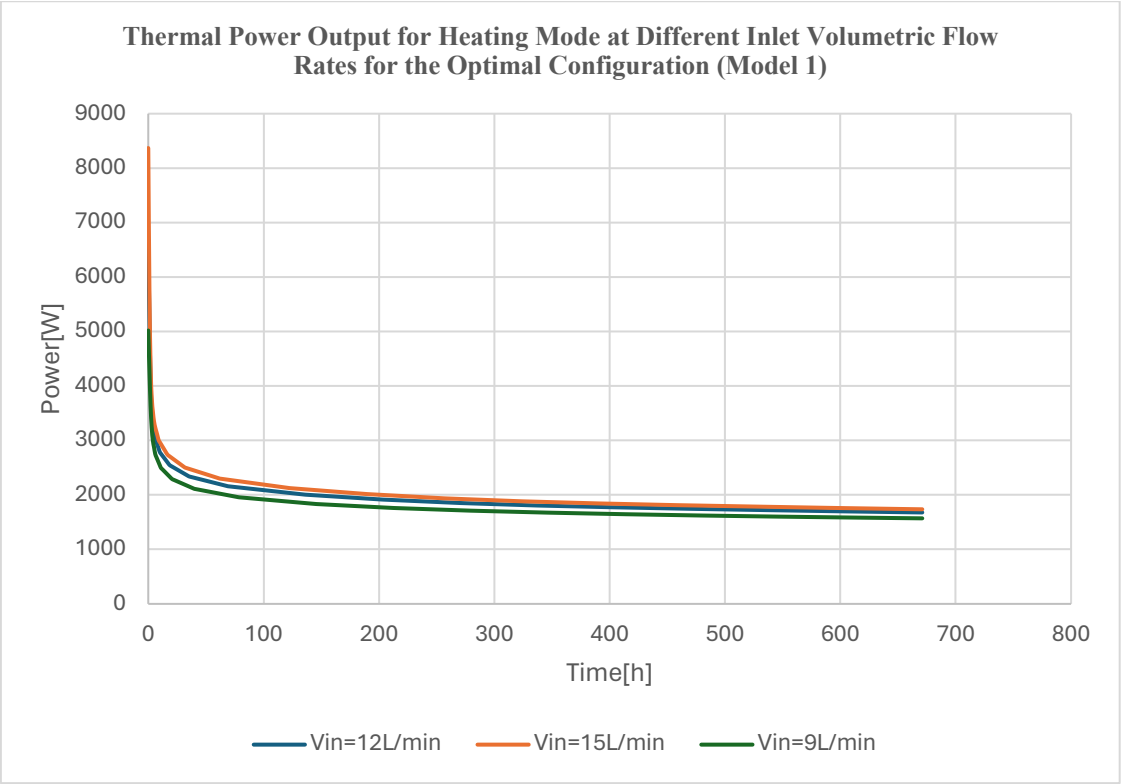

Figure 4. 14 ***Thermal Power Output for Heating Mode at Different Inlet Volumetric Flow Rates for the Optimal Configuration (Model 1)***

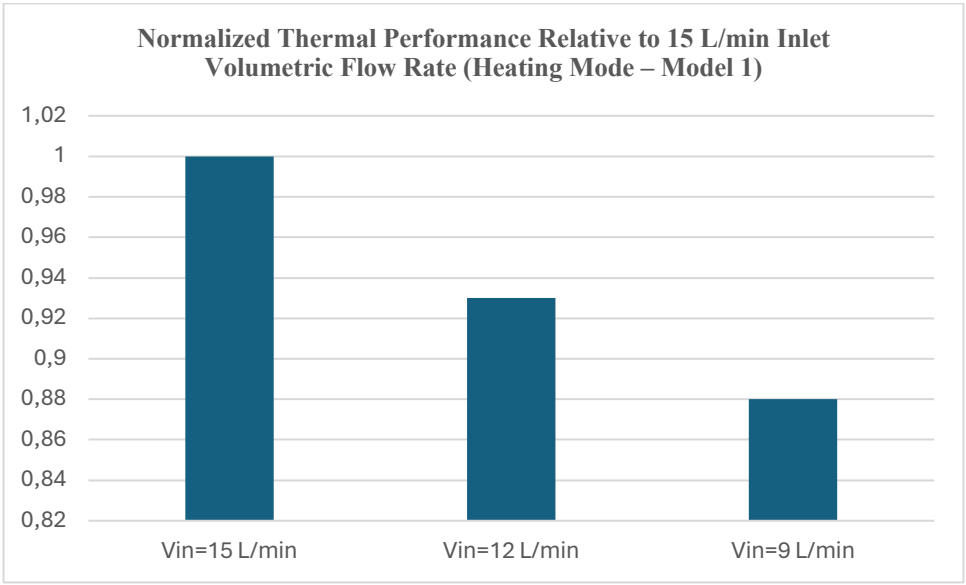

Figure 4. 15 ***Normalized Thermal Performance Relative to 15 L/min Inlet Volumetric Flow Rate (Heating Mode – Model 1)***

Figure 4.15 presents the normalized thermal performance of Model 1 under heating mode, with results scaled relative to the performance at 15 L/min inlet volumetric flow rate. The plot shows a clear decrease in normalized thermal performance as the inlet flow rate decreases. This indicates that higher flow rates lead to improved thermal efficiency, as more fluid is circulated, and greater thermal energy is extracted from the ground. At higher flow rates, although the residence time is reduced, the increased mass flow compensates by carrying more heat, resulting in better overall performance. Conversely, lower flow rates reduce the total energy transported by the fluid, leading to lower thermal output.

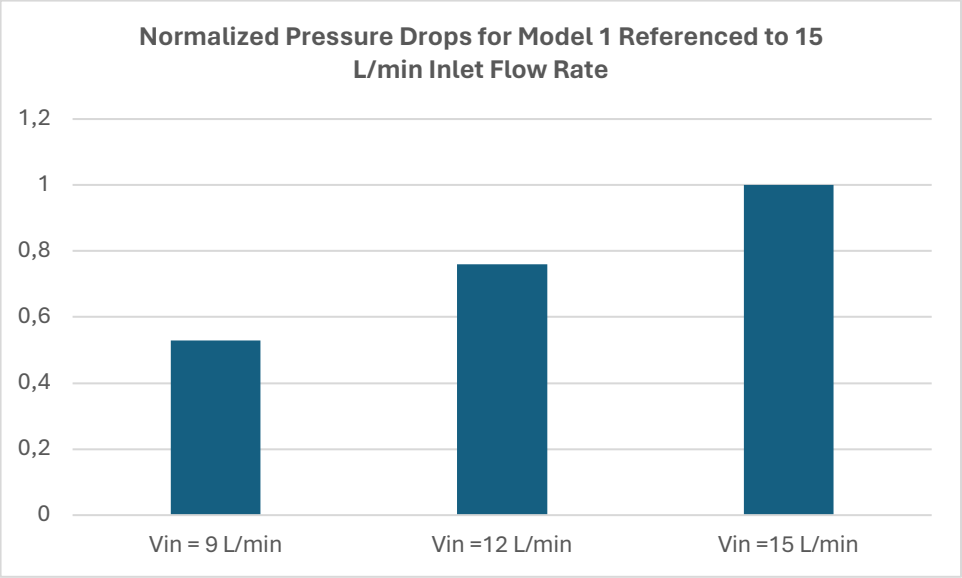

Figure 4. 16 **Normalized Pressure Drops for Model 1 Referenced to 15 L/min Inlet Flow Rate**

The chart illustrates the normalized pressure drops for Model 1 at inlet volumetric flow rates of 9, 12, and 15 L/min. All values are scaled relative to the pressure drop observed at 15 L/min, which is set to 1. As shown, the pressure drop increases with the inlet flow rate due to the quadratic relationship between velocity and pressure loss. This analysis highlights the trade-off between higher flow rates (which improve heat exchange) and the increased pumping power required due to higher pressure drops.

The corresponding absolute pressure drop values for each inlet flow rate are:

- 9 L/min: 251.65 Pa
- 12 L/min: 354.7 Pa
- 15 L/min: 465.6 Pa

4.4 Termus and Geothermus Results

Scenario	Apartment name	AreaN [m^2]	VlmN [m^3]	P_h (Heating power) [W]	P_c (Cooling power) [W]	Annual heating Q_h [kWh]	Annual cooling Q_c [kWh]	L_h [m] * number of systems	L_c [m]* number of systems
1	Sub 1	70.6	194.14	5563	4864	8832.55	-444,85	57 *2	50*2
	Sub 10	70.57	194.07	5512	4761	8531.78	-532,94	59*2	47*2
	Sub 3	70.6	194.14	5947	5121	9877.97	-531,5	67*2	51*2
	Sub 4	70.57	194.07	5710	5032	9404,4	-513,63	62*2	50*2
2	Sub 1	70.6	194.14	4522	4566	6592.75	-594,99	45*2	50*2
	Sub 10	70.57	194.07	4421	4478	6251,68	-749,15	48*2	40*2
	Sub 3	70.6	194.14	4909	4843	7638.88	-709,32	53*2	51*2
	Sub 4	70.57	194.07	4600	4765	7076	-733,49	47*2	51*2
3	Sub 1	70.6	194.14	5563	4864	8832.55	-444,85	57*2	50*2
	Sub 10	70.57	194.07	5512	4761	8531.78	-532,94	59*2	47*2
	Sub 3	70.6	194.14	4196	4160	5528.71	-883,97	82*1	47*2
	Sub 4	70.57	194.07	3959	4072	5057.76	-876,9	73*1	46*2
4	Sub 1	70.6	194.14	4522	4566	6592,75	-594,99	45*2	50*2
	Sub 10	70.57	194.07	4421	4478	6251,68	-749,15	85*1	40*2
	Sub 3	70.6	194.14	3161	3878	3334,5	-1234,18	57*1	47*2
	Sub 4	70.57	194.07	2864	3820	2814,96	-1258,75	47*1	48*2

Table 4. 1 ***Heating and Cooling Performance of Apartments under Different Insulation Scenarios Simulated in Termus***

The results obtained from Termus simulations under four different insulation scenarios :

1. no insulation
2. wall insulation only
3. roof insulation only
4. combined wall and roof insulation

highlight the significant impact of building envelope improvements on energy performance. In the baseline case (Scenario 1), apartments exhibited the highest heating power demand (P_h) and annual heating energy consumption (Q_h), with Sub 3 reaching a peak Qh of 9877.97 kWh and P_h of 5947 W. Regarding cooling performance, the highest instantaneous cooling power (Pc) was observed in Scenario 1, Sub 3 (5121 W), while the greatest annual cooling energy consumption (Qc) occurred in Scenario 4, Sub 4, reaching -1258.75 kWh."

The introduction of wall insulation alone (Scenario 2) led to a noticeable reduction in heating demand across all units. Similarly, applying only roof insulation (Scenario 3) also yielded considerable energy savings. However, the most effective performance was observed in Scenario 4, where both wall and roof insulation were applied simultaneously.

These results provide the necessary thermal energy demand data that must be entered into Geotermus to simulate the geothermal heat exchanger performance. By using the peak heating power (P_h) and annual heating energy (Q_h) values from each scenario, Geotermus allows for the design of an appropriate geothermal system specifically, calculating the required borehole depth to satisfy the heating demand of the building under each insulation strategy.

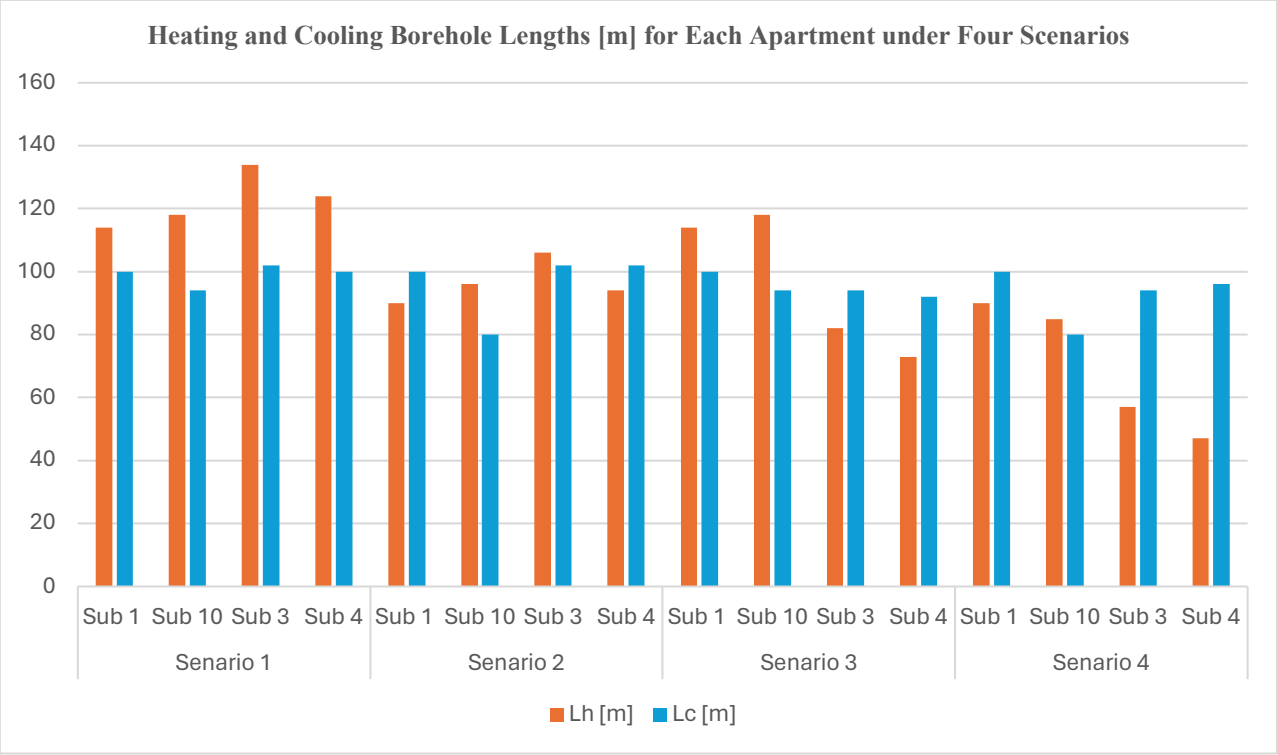

Figure 4. 17 ***Heating and Cooling Borehole Lengths [m] for Each Apartment under Four Scenarios***

Figure 4.17 shows how the required borehole lengths for heating (Lh) and cooling (Lc) change for four different insulation scenarios across four apartments (Sub 1 to Sub 4). This shows that in well-insulated buildings, cooling may require longer boreholes than heating, especially when heat losses are minimized.

In the first scenario, there is no insulation, so both Lh and Lc are high for all apartments. In the second scenario, wall insulation is added. This reduces both lengths slightly in all apartments because walls lose less heat.

In the third scenario, only roof insulation is applied. This mostly affects Sub 3 and Sub 4, which are on the top floor and directly under the roof. That's why these two apartments show a bigger reduction compared to Sub 1 and Sub 10.

In the fourth scenario, both wall and roof insulation are used. This gives the best results, with the lowest borehole lengths especially for Sub 3 and Sub 4. These results show that both insulation and

the apartment's vertical position (whether it's under the roof or not) are important in determining how much energy is needed, and therefore how deep the boreholes must be.

When considering the four apartments as part of a shared geothermal system, the required borehole lengths change depending on the level of insulation applied.

Scenario	AreaN [m^2]	VlmN [m^3]	P_h (Heating power) [W]	P_c (Cooling power) [W]	Annual heating Q_h [kWh]	Annual cooling Q_c [kWh]	L_h [m] * number of systems	L_c [m]* number of systems
1	282.34	776.42	22732	19738	36646.7	-2022,92	6*85	5*76
4	282.34	776.42	14968	16742	18993.89	-3837.07	4*73	5*76

Table 4. 2 ***Comparison of Heating and Cooling Loads and Borehole Configuration for Scenarios 1 and 4 With and Without Insulation***

In the first scenario (no insulation), the system must meet high heating and cooling demands. As a result, the required borehole configuration is:

Heating (L_h): 6 boreholes, each 85 meters → Total = 510 m

Cooling (L_c): 5 boreholes, each 76 meters → Total = 380 m

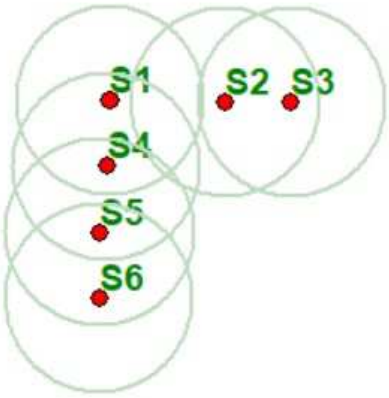

Figure 4. 18 ***Configuration of Six Coaxial Geothermal Probes Used in Geotermus for Heating Mode***

As shown in Figure 4.18, six coaxial geothermal probes were arranged in the heating configuration within Geotermus, with a spacing of 7 meters between each borehole

In the 4th scenario, with both wall and roof insulation applied, the thermal load is reduced, especially for heating. The system configuration becomes:

Heating (L_h): 4 boreholes, each 73 meters → Total = 292 m

Cooling (L_c): remains the same → 5 boreholes, each 76 meters → Total = 380 m

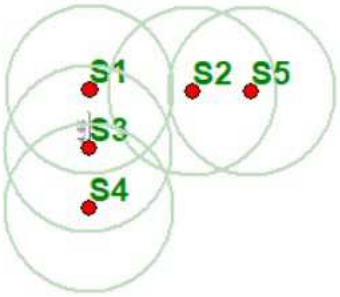

Figure 4. 19 **Configuration of Five Coaxial Geothermal Probes Used in Geotermus for Cooling Mode**

Figure 4.19 shows five coaxial geothermal probes were arranged for the cooling mode in Geotermus, maintaining a distance of 7 meters between each borehole. This comparison shows that heating demand benefits significantly from insulation, allowing a 43% reduction in total heating borehole length (from 510 m to 292 m). Meanwhile, cooling demand slightly increases with enhanced insulation, likely due to the reduced ability of the building to dissipate internal and external heat gains during warmer periods. Roof insulation, while beneficial in reducing heating losses, may trap heat during summer, particularly in top-floor units.

These results demonstrate that when apartments are combined into a single geothermal system, thermal insulation especially roof insulation plays a crucial role in reducing the system size for heating, while the cooling side may require separate strategies for optimization. However, in practice, the choice between centralized and individual geothermal systems depends on various factors. Centralized systems offer better efficiency and lower installation costs per unit but may face challenges in balancing loads and managing shared responsibilities. On the other hand, individual systems provide independent control but are often less space and cost-efficient. These trade-offs should be considered during the design phase. This insight supports the case for building envelope upgrades as a cost-effective way to reduce geothermal installation depth and costs in shared systems.

5

Conclusions and future works

In this work, a detailed numerical and building-level investigation was conducted to evaluate the thermal and hydraulic performance of coaxial borehole heat exchangers (CBHEs), combining COMSOL Multiphysics simulations with building energy modelling using Termus and sizing of a geothermal field with Geotermus. The COMSOL analysis explored multiple CBHE configurations with systematic variations in pipe diameters and flow rates, simulating a realistic 85 m deep borehole under the climatic conditions of Padova. Both heating and cooling scenarios were considered, with parametric studies involving constant volumetric flow rates.

The COMSOL model was validated against operational data from a CBHE system in Mechelen, Belgium. Validation showed strong agreement between simulated and real return fluid temperatures, with statistical indicators (CV = 9.79%, MBE = –1.81%) falling within acceptable ASHRAE limits, confirming the model's reliability.

The simulation results demonstrated that Model 1, with the largest inner pipe diameter and smallest annular gap (Ø63 mm – Ø88.9 mm), delivered the best thermal performance in both heating and cooling. This was attributed to reduced heat losses in the smaller annular region and improved return fluid temperature due to enhanced interaction with the surrounding ground. Velocity and temperature profiles confirmed the expected thermal behaviour and the influence of subsurface depth on heat exchange.

Parametric analysis further showed that lower inlet flow rates (e.g., 9 L/min) improved heat exchange by allowing longer residence times within the borehole. However, very low flow rates reduced thermal power output. Therefore, flow rate optimization is essential to achieve a balance between energy extraction and system efficiency.

In parallel, the Termus and Geotermus simulations provided an applied perspective on energy demand and geothermal system sizing at the building level. Using four apartment units as a case study, various insulation scenarios were analysed. It was observed that wall insulation reduced both heating and cooling demands in all units, while roof insulation significantly affected only the upper-floor apartments (Sub 3 and Sub 4). When each apartment was considered independently, borehole lengths varied between 45 m and 62 m depending on energy demand and insulation type. The most noticeable reductions occurred in Sub 3 and Sub 4 under the full insulation scenario (wall + roof), confirming the importance of exposure to external surfaces in thermal load reduction.

A final shared-system analysis revealed that, when considering all four apartments together, the required borehole length dropped significantly for heating from 6*85 m in the non-insulated case to 4*73 m in the fully insulated case while the cooling side remained constant at 5*76 m.

In conclusion, this study confirms that increasing the inner pipe diameter, reducing the annular gap, and selecting appropriate flow rates are critical to optimizing CBHE thermal performance. Additionally, integrating system-level building analysis through Termus and Geotermus provides a valuable link between equipment design and building energy needs. These combined insights support more efficient CBHE design, reduced installation depth, and better alignment of geothermal systems with actual heating and cooling demands.

To further enhance the design and applicability of coaxial borehole heat exchangers, future work can focus on the following areas:

Test the same CBHE system in different cities with colder or hotter climates, to see how weather affects the performance of the system.

Try other types of insulation (such as floor insulation or double-glazed windows) in the building model, to see how much they reduce heating and cooling demands.

Combine the geothermal system with solar panels, to reduce electricity costs and improve energy sustainability.

Do long-term simulations (for example, over 10 or 20 years) to understand how the ground temperature changes over time and how it affects system performance.

Compare the coaxial system with other geothermal systems like U-tube systems, to see which one works better in similar buildings.

References

[1] European Commission, “Stepping up Europe’s 2030 climate ambition: Investing in a climate-neutral future for the benefit of our people,” COM(2020) 562 final, Brussels, 2020.

[2] Eurostat, “EU imports of goods fell by 16% in 2023,” Eurostat News, Mar. 5, 2025. [Online]. Available: https://ec.europa.eu/eurostat/web/products-eurostat-news/w/ddn-20250305-1

[3] Dalhousie University, “Geothermal Energy Research,” Sustainable Energy Research, [Online]. Available: https://www.dal.ca/sites/sustainable-energy/research-initiatives/GeothermalEnergyResearch.html.

[4] Sustainability Directory, “Low-Enthalpy Geothermal,” [Online]. Available: https://energy.sustainability-directory.com/term/low-enthalpy-geothermal/.

[5] O. Vytyaz, A. Zimovets, V. Pivovarov, and O. Rachkov,”*ResearchGate*, 2016. [Online]. Available: https://www.researchgate.net/figure/Schemes-of-the-borehole-heat-exchangers-design-a-single-U-tube-b-double-U-tube-c_fig1_306208661

[6] J. Raymond, R. Therrien, and L. Gosselin, "A review of thermal response test analysis using pumping tests and modeling approaches," Renewable and Sustainable Energy Reviews, vol. 44, pp. 727–736, 2015, doi: 10.1016/j.rser.2014.12.034.

[7] M. Quaggiotto, A. Zarrella, G. Emmi, and M. De Carli, "9-year simulation of a ground source heat pump system using shallow borehole heat exchangers: Comparison between coaxial and U-tube configurations," Applied Thermal Engineering, vol. 148, pp. 602–612, 2019, doi: 10.1016/j.applthermaleng.2018.11.055.

[8] B.D. Wood, X. Liu, and R. Southard, "Comparison of coaxial and U-tube borehole heat exchangers in groundwater flow," Geothermics, vol. 42, pp. 123–131, 2012, doi: 10.1016/j.geothermics.2012.01.001.

[9] J. Acuña and B. Palm, "Distributed thermal response test: A new method to infer in situ effective borehole thermal resistance," Applied Energy, vol. 109, pp. 312–320, 2013, doi: 10.1016/j.apenergy.2013.04.034.

[10] J. Raymond, S. Mercier, and L. Nguyen, “Designing coaxial ground heat exchangers with a thermally enhanced outer pipe,” *Geothermal Energy*, vol. 3, no. 7, 2015, doi: 10.1186/s40517-015-0027-3.

[11] M. Iry and R. Rafee, "Parametric study of the coaxial ground heat exchanger performance: Influence of pipe geometry and flow conditions," Energy and Buildings, vol. 183, pp. 377–387, 2019, doi: 10.1016/j.enbuild.2018.11.037.

[12] R. Morchio and M. Fossa, "Evaluation of optimal geometries for coaxial borehole heat exchangers in high conductivity soils," Renewable Energy, vol. 135, pp. 680–691, 2019, doi: 10.1016/j.renene.2018.12.049.

[13] M.N. Yekoladio, C.Z. Kimambo, and R.T. Kivaisi, "Numerical simulation of a coaxial borehole heat exchanger in layered geological formations," International Journal of Energy and Environmental Engineering, vol. 4, no. 1, pp. 1–9, 2013, doi: 10.1186/2251-6832-4-19.

[14] K. Oh, S. Lee, S. Park, S.-I. Han, and H. Choi, "Field experiment on heat exchange performance of various coaxial-type ground heat exchangers considering construction conditions," Renewable Energy, vol. 144, pp. 84–96, 2019, doi: 10.1016/j.renene.2019.06.018.

[15] A. Zarrella, G. Emmi, and M. De Carli, "Experimental investigation and numerical modeling of a novel coaxial borehole heat exchanger," Energy and Buildings, vol. 43, no. 12, pp. 3262–3270, 2011, doi: 10.1016/j.enbuild.2011.08.002.

[16] Y. Pan, Z. Ma, and Z. Zhang, "A new analytical model for thermal performance prediction of coaxial borehole heat exchangers," Renewable Energy, vol. 136, pp. 1853–1861, 2019, doi: 10.1016/j.renene.2019.01.065.

[17] J. Oliver and H. Braud, "Thermal exchange to earth with concentric well pipes," Transactions of ASAE, vol. 24, no. 4, pp. 906–910, 1981.

[18] A. Pan, L. Lu, P. Cui, and L. Jia, "A new analytical heat transfer model for deep borehole heat exchangers with coaxial tubes," International Journal of Heat and Mass Transfer, vol. 141, pp. 1056–1065, 2019.

[19]: Climate.Top, 2025. [Online]. Available: https://www.climate.top/italy/padova/

[20] Il Bo Live, “Energia geotermica, tra promesse di futuro e opportunità mancate,” Università di Padova, 21 luglio 2023. [Online]. Available: https://ilbolive.unipd.it/it/news/societa/energia-geotermica-promesse-futuro-opportunita

[21] G. Mezzasalma, L. Pockelé, S. Contini, J. Vercruysse, A. Galgaro, G. Emmi, D. Righini, and M. Psyk, "Evaluation of performance in demonstration site N°3: Residential house, Belgium (Deliverable D6.3)," Cheap-GSHPs Project, European Commission, Grant Agreement No. 657982, WP6, pp. 1–60, 2018.

[22] ACCA Software, “Certificazione Energetica con Termus,” ACCA, 2024. [Online]. Available: https://www.acca.it/software-certificazione-energetica

[23] ASHRAE, *Geothermal Heating and Cooling: Design of Ground-Source Heat Pump Systems*, American Society of Heating, Refrigerating and Air-Conditioning Engineers, 2018.

[24] Domusgaia and NIBE, "Listocatalogo 2023 (Versione 2.0)," Domusgaia, 2023.

[25] VITO, “Geothermal Energy in Belgium,” Vlaamse Instelling voor Technologisch Onderzoek (VITO), 2023. [Online]. Available: https://vito.be/en/geothermal-energy/geothermal-energy-belgium.